FI-11-05

*Stapp Car Crash Journal,* Vol. 47 (October 2003), pp. 323-348

2003-22-0015

# Thoracic Injury Criterion for Frontal Crash Applicable to All Restraint Systems

Audrey Petitjean and Pascal Baudrit
Centre Européen d'Etudes de Sécurité et d'Analyse des Risques, Nanterre, France

Xavier Trosseille
LAB PSA-Renault, Nanterre, France

**ABSTRACT** – For several years now, car manufacturers have made significant efforts in the field of thoracic protection. After first limiting the forces in the shoulder belt to 6 kN, these forces are now usually limited to 4 kN, with airbags intentionally designed to absorb the surplus of energy. If this technology is rewarded by a considerable improvement in safety on the road, it remains penalized by the usual biomechanical criteria, when calculated on the Hybrid III and if applied to all restraint systems.
To remedy this problem, a new criterion, valid in all the current restraint configurations (belt, airbag only or airbag and belt) is proposed. It is based on the measurement of the shoulder belt forces and of the central deflection and consequently is directly applicable to the current dummy model (Hybrid III). The use of shoulder belt forces allows the separation of the belt and airbag contributions to the deflection. A weighted criterion is calculated from these deflections, taking into account the different risks associated with a belt and an airbag for the same deflection. This new criterion was developed using 65 simulations on the LAB human model and validated by means of 48 sled tests from the literature, consisting of Hybrid III dummy and PMHS tests performed in similar configurations.
This paper describes the logic behind the development of the criterion and gives all the parameters used as well as the elements of validation.

**KEYWORDS** – thorax, injury criterion, frontal crash, Hybrid III

## INTRODUCTION

Crash investigation studies allow the identification of the types of injury sustained in frontal impacts and show that the reduction of thoracic injuries remains an important concern, particularly for elderly occupants.

Several thoracic injury criteria have been developed in order to predict thoracic risk and in order to evaluate the effectiveness of new restraint systems. As restraint systems are evaluated using dummies, the injury criteria were determined using measurements made on the dummy. The first thoracic criteria developed using blunt impact tests were the chest deflection and a linear combination of chest compression and age and were applicable for steering wheel-like loading (Kroell et al. (1971), Neathery et al. (1975)). Mertz et al. found that the chest compression criterion was also applicable to predict the thoracic risk under belt loading but that the chest compression/risk relationship differed in that the chest compression sustainable for a 50% AIS3+ risk is lower under belt loading (50 mm, Mertz et al. (1991)) than under blunt loading (61 mm, Mertz et al. (1997)). The chest compression limit determined with belt loading was used as the limit for localized loading, and the one determined with blunt loading as the limit for distributed loading, including airbag loading.

Kallieris et al. (1996) and Crandall et al. (1996) showed that combined belt and airbag restraint offered more effective thoracic protection, especially with a load-limiting belt. The lowering of the shoulder belt load allows the thoracic injury risk to be reduced. At the same time, the airbag avoids the increase of the head and neck injury risks due to greater torso motion. Petitjean et al. (2002) confirmed the better effectiveness of a combined restraint (4 kN load-limiting belt plus airbag) compared to a shoulder belt restraint (6 kN load-limiting belt). However, this effectiveness was not illustrated by the thoracic

compression criterion. This may be due to the fact that only one deflection limit is considered for two loading configurations, while the sternal deflection tolerated depends on the loading type.

Lau et al. (1986) found that the viscous criterion characterized the thoracic injury risk for chest deformation velocities above 3 m/s. However, this criterion did not confirm the greater effectiveness of the 4 kN load-limiting belt and airbag compared to the 6 kN load-limiting belt (Petitjean et al (2002)).

Kuppa et al. (1998) proposed the combined thoracic injury criterion in order to predict thoracic risk, whatever the restraint system. However, as this criterion includes the upper spine acceleration, it is dependent on possible head impact on car components (Petitjean et al (2002)). A new criterion, independent of the head kinematics and valid in all the current restraint configurations (belt, airbag only or airbag and belt) is therefore proposed. It is based on the measurement of the shoulder belt forces and of the central deflection and consequently is directly applicable to the currently used frontal dummy (Hybrid III). The use of shoulder belt forces allows the separation of the belt and airbag contributions to the deflection. A weighted criterion is calculated from these deflections, taking into account the different risks associated with a belt and an airbag for the same deflection. It is assumed that even if the risk associated with the shoulder belt force may be influenced by the geometry, its use for balancing the contribution of different loading sources is better than using directly the central chest deflection, whatever the restraint type.

This new criterion was developed using 65 simulations on the human model of the LAB presented by Lizee et al. (1998) and validated with 48 sled tests from the literature and consisting of Hybrid III dummy and PMHS (Post Mortem Human Subjects) tests performed in similar configurations.

**Criterion Principle**

Here is explained the criterion principle through its main steps. More detailed analysis is developed further in the Methods section for the validation and calculation of the criterion on the one hand for the human body model and on the other hand for Hybrid III dummy.

The risk of injury to a chest subjected to the load of a belt-only can be estimated by means of the sternal deflection. Also, the risk of injury to a chest loaded by an airbag only or an impactor can be estimated by the thoracic deflection. However, the levels of deflection corresponding to a given injury risk differ according to whether the load is localized or distributed (according to Mertz et al. (1991), 50 mm for a belt and according to Mertz et al. (1997), 61 mm for an impactor correspond to the same risk of 50 % of AIS3 +). To address this problem, one could assume the risk for belt loading when combined loading takes place. This would be a conservative approach as the injury risk from combined loading is lower than that from belt loading alone. However, this approach would not encourage improvements of restraining systems by decreasing belt loads to allow airbags to carry more of the load. In particular, this would not discriminate two systems (6 kN versus 4 kN and airbag) which demonstrate very different effectiveness on the road (Foret-Bruno et al. (2001)).

So that a given level of risk corresponds to a single deflection, whatever the load type, it is proposed to normalize the deflection associated to the distributed load (airbag loading) so that it corresponds to the deflection associated to a localized load (belt loading) giving the same risk. The normalization factor ($f_n$) was determined for 50% risk. It corresponds to the ratio of the localized deflection value at 50% risk to the distributed deflection value at 50% risk.

By applying this normalization to all the risks, a single risk curve is obtained, superposing localized load risk curve and the distributed load risk curve. This single risk curve can then be used for any type of restraint.

In the case of a combined restraint, a part of the total deflection results from the localized loading by the belt and another part results from the distributed loading by the airbag. If the total deflection is associated with the risk corresponding only to localized loading, the risk predicted for the combined restraint will be overestimated (Petitjean and al. (2002)). On the other hand, if the total deflection is associated with the risk corresponding only to distributed loading, the risk predicted for the combined restraint will be underestimated.

The difficulty is to attribute a part of the risk to the localized loading and another part of the risk to the distributed loading. The risk due to a localized load is obtained according to the maximal deflection caused by the belt; the risk due to a distributed load is obtained according to the maximal deflection caused by the airbag. It is therefore necessary to separate the contribution of the belt from that of the airbag in the

total deflection measured during the crash in order to calculate a risk adapted to a combined restraint.

To calculate the maximal deflection resulting from the belt, it is possible to use the belt force measured during the crash. Indeed, a relationship between the shoulder belt force and the maximal deflection can be determined in the case of a belt restraint only. A relationship of the following form was found to correctly model the behavior of the chest loaded by a belt-only restraint:

$$F_{belt}(t) = k\, d_l(t) + c\, v_l(t) \qquad \text{(Equation 1)}$$

where k and c are the linear stiffness and the damping respectively and $d_l(t)$ and $v_l(t)$ are the deflection and the rate of deflection respectively.

The maximal deflection was then calculated by resolving the differential Equation 1 with a Runge-Kutta method. It is to notice that the k and c coefficients could be constant and equal for all belt-only test configurations, as for the human body model as shown further in this article, or constant for a given crash configuration but variable according to the belt-only test configurations, as for the Hybrid III dummy for which the stiffness is a function of the shoulder belt force, as shown below.

Equation 1 was optimized for each test to minimize the mistakes in calculation of the maximal deflection caused by the belt.

The use of this relationship thus allows the estimation of the maximal deflection caused by the belt, even in the case of a combined restraint. In a combined restraint configuration, the total deflection is equal to the sum of the deflections coming from both load types (localized and distributed). The maximal deflection produced by the airbag is then deduced by simple subtraction of the deflection produced by the belt in the total deflection measured during the crash, as indicated by Equation 2.

$$d_d(t) = d_t(t) - d_l(t) \qquad \text{(Equation 2)}$$

where $d_d(t)$ is the maximal distributed deflection, $d_t(t)$ is the maximal deflection measured, $d_l(t)$ is the maximal localized deflection calculated.

To use the injury risk curve valid for any type of restraint, a single deflection taking into account the maximal deflection produced by the belt and the maximal normalized deflection produced by the airbag has to be calculated. This deflection will be named "equivalent". The combination of the two types of deflection in the calculation of the equivalent deflection represents the form of the risk resulting from these two types of load and must be determined.

Injury mechanisms associated to the belt on one hand and to the airbag on the other hand are different. The airbag does not create concentrated areas of strain, but provokes a global deformation of the chest. Rib fractures are typically found at the lateral part of the chest. In contrast, belt loading creates above all local strains and deformations typically resulting in rib fractures along the path of the belt (Yoganandan et al. (1993), Kallieris et al. (1994)). Nevertheless, this local loading also results in a global loading component connected to the force applied by the belt to the chest and also provoking a global deformation.

As a consequence, injury mechanisms being different, the risks connected to these two loadings do not cumulate directly ($d_{eq}(t) = d_l(t) + f_n\, d_d(t)$, dashed line in Figure 1). They are not completely separated either because the belt-only restraint generates global deformations similar to those generated by the airbag ($d_{eq}(t) = d_l(t)$ and $d_{eq}(t) = f_n\, d_d(t)$, continuous line in Figure 1). It is therefore necessary to define the best scenario that will represent the most realistic overlap of risks. Equation 3, which is an intermediate position, was chosen as a first approach to model the total risk to the chest regardless of the restraint configuration (thick line in Figure 1).

$$d_{eq}(t) = (d_l^2(t) + (f_n\, d_d(t))^2)^{1/2} \qquad \text{(Equation 3)}$$

where $d_{eq}(t)$ is the equivalent deflection, $d_l(t)$ is the maximal deflection caused by the localized loading, $d_d(t)$ is the maximal deflection caused by the distributed loading and $f_n$ is the normalization factor.

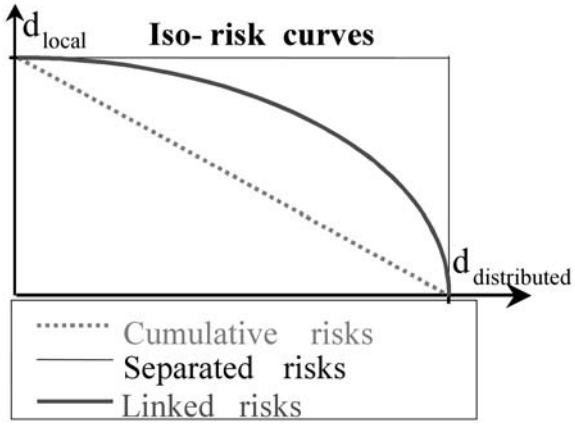


**Figure 1: injury risk combination for local and distributed loading**

In order to construct risk curves corresponding to the new criterion, shoulder belt load and thoracic

deflection measurements associated with injuries were needed.

The criterion was first developed using a numerical human body model presenting rib fractures. Use of the model allowed the shoulder belt load and thoracic deflection measurements as well as the injuries for the same numerical crash configuration to be obtained. The criterion was subsequently transferred to the physical Hybrid III dummy. Shoulder belt load and thoracic deflection measurements were obtained from dummy crash tests in various configurations. Injuries obtained from PMHS tests performed in similar conditions were associated to these measurements.

**Statistical Methods**

*Risk curve construction with certainty method*
The distribution of the risk as a function of the criterion being unknown, a non-parametric estimation method should be used to determine the risk curve. Moreover, the data used is always right and left censored. Test data is right censored for an AIS3+ thoracic risk curve when the injury is lower than AIS3 and therefore when it is not possible to predict for which criterion value the injury would have been AIS3. Test data is left censored when the injury is higher than AIS3 and when it is not possible to determine for which criterion value the injury was equal to AIS3. The certainty method allows one to take into account the censored data and is particularly adapted when the data is sparse (one or two tests for each range of criterion values) (Mertz et al. (1996), Nusholtz et al. (1999)). The certainty method was used to construct all the risk curves presented in this article.

*C statistic index*
The appropriateness of a criterion for prediction of a risk can be assessed by constructing a risk curve as a function of this criterion and calculating the percentage of concordance and discordance and the c statistic index.

In order to determine the percentage of concordance/discordance, each pair of observations including one observation without injury (0) and one with injury (1) is studied. If the risk predicted by the criterion is lower (at a threshold of 0.002) for the observation without injury than for the one with injury, the pair of observations is concordant. Otherwise, it is discordant. The c statistic index is a combination of the number of concordant/discordant pairs among all pairs of observations with different responses in the analysis data:

$c = (nc + 0.5 * (t- nc – nd))/t$, where nc is the number of concordant pairs, nd the number of discordant pairs and t the number of pairs of different responses.

A c statistic value equal to 0.5 indicates an inappropriate criterion to predict the risk while a c value equal to 1 indicates a perfect appropriateness. The higher the c value is, the better the criterion predicts the risk.

**Human Body Model**

*Human body model*
The human body model used was described by Lizee et al. (1998). The ribcage is made up of ribs, intercostal ligaments, sternum and costal cartilage (Figure 2). The rib part is composed of triangular shells characterized by an elastic material law. The biofidelity of the thorax in terms of global behavior and kinematics was validated with impactor and shoulder belt loading tests.

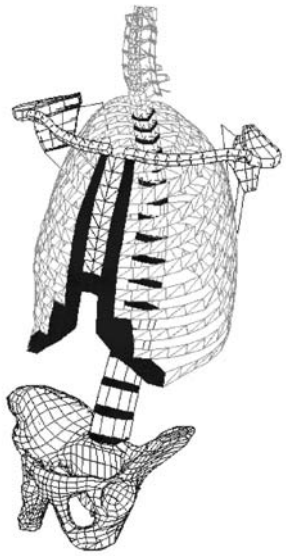

**Figure 2: Human body model thorax**

This model was modified in order to demonstrate the rib fractures, applying an elasto-plastic material law with rupture, as described by Besnault et al. (1998) for the pelvis. A rib fractures when a shell element presents a plastic deformation over 3%. The human body model biofidelity was not altered by these modifications. This injury model allows the determination of a risk curve as a function of the equivalent deflection.

The risk curves were constructed for a risk of 7 rib shells presenting a plastic deformation over 3%. This level was chosen because of the distribution of cases

with and without injuries, which has to be balanced for all the restraint configurations (Figure 3).

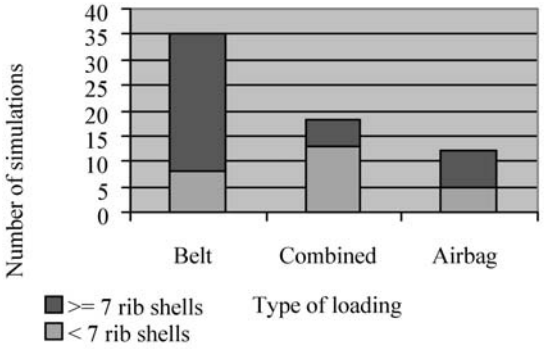


**Figure 3: Number of simulations based on the number of rib shell fractures, according to the restraint system**

The human body model used did not intend to present rib shell fractures at locations similar to those observed on PMHS when loaded by a belt or an airbag restraint. However, the patterns of stress/strain found on the thorax are globally consistent with those observed in real-world crash configurations or in PMHS tests, even if the fractures were not exactly reproduced. Therefore, a deeper analysis would be required in order to reproduce rib shell fracture locations similar to PMHS rib fracture locations. Otherwise, it was verified that the human body model correctly reproduces quantitatively the rib fractures. In particular, it was verified that the number of rib shell fractures was higher with a 6 kN load-limiting belt restraint than with a 4 kN load-limiting belt and airbag for a given crash configuration (i. e. for identical deceleration law, initial velocity, crash angle). As an example, the number of rib shell fractures is presented for three configurations of crash simulation with these two restraints in Table 1.

**Table 1: Number of rib shell fractures on the human body model for the 6 kN load-limiting belt restraint and the 4 kN load-limiting belt and airbag restraint.**

| Rib shell fractures with 6 kN load limiting belt | Rib shell fractures with 4 kN load limiting belt and airbag |
|---|---|
| EH_CEI84: **24** | EH_CEI29: **6** |
| EH_CEI48: **22** | EH_CEI41: **9** |
| EH_CEI44: **34** | EH_CEI17: **15** |

As a consequence, the human body model was considered to be sufficiently pertinent to reproduce the main phenomenon concerning the thoracic injury criterion (i. e. the difference of deflection tolerated according to the loading configuration) in order to be useful for the determination of a new thoracic injury criterion, whatever the rib shell fracture localization.

Mertz et al. proposed a sternal deflection of 50 mm for a 50% AIS3+ risk under localized loading (Mertz et al. (1991)) and of 61 mm for distributed loading (Mertz et al. (1997)). It was therefore verified on the human body model that the sternal deflection corresponding to a given risk was lower under localized loading than under distributed loading. For a risk of 7 rib shell ruptures, the sternal deflection was 42 mm under shoulder belt loading and 72 mm under airbag loading (Figure 4).

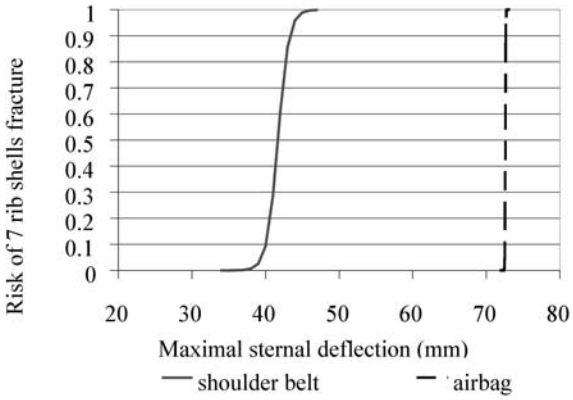


**Figure 4: Human body model risk curve as a function of the maximal sternal deflection**

As a consequence, the use of the plastic deformation limit of the rib shell as a rupture criterion allows correct representation of the greater sternal deflection tolerated with a distributed load compared to a localized load for a given risk.

As the human body model biofidelity was verified and it correctly represents the main phenomenon relevant to the injury criterion for all restraint systems, it can be used as a tool to determine the principle of a new thoracic injury criterion.

The use of the human body model is advantageous in that a single individual is considered. Indeed, the human body model presents a given bone strength, which is represented by the plastic deformation limit of the rib shells. It allowed us to predict the thoracic risk for a single individual. Therefore, no anthropometric dispersion (mass and age) would modify the risk one way or another thus avoiding dispersion of the risk curve. As a consequence, the risk curve would present a single criterion threshold separating completely the cases of low level of injury

from those of high level of injury if the criterion is pertinent.

*Test Configuration*

In order to evaluate the appropriateness of the new criterion, it was necessary to apply it in a large range of configurations. The simulation analysis data created for this purpose included simulations for which parameters like the restraint type, deceleration pulse and initial velocity, varied. The description of the simulation configurations is presented in appendix, in TableA 1, TableA 2, TableA 3 and in FigureA 1, FigureA 2, FigureA 3.

The simulated restraints were belt-only restraint (shoulder and lap), combined restraint (shoulder and lap belt plus airbag) and airbag only restraint. The belt-only and combined restraints were used in sled test simulations. The range of sled initial velocities was from 22 to 56 km/h; the range of maximal sled decelerations was from 7 to 21 g, the crash angle was between +15° and –15°. Most of the simulations under airbag loading were simulated using an airbag fixed on a plate "impacting" the human body model, the plate having a given mass and a given initial velocity and the human body model being free to translate rearwards. It was verified the maximum and duration of loading were consistent with those observed during a car crash with airbag-only restraint. The characteristics of each restraint varied. Concerning the belt-only restraint, the load limiter, the shoulder belt anchorage and the knee bolster stiffness varied. Concerning the combined restraint, the load limiter and the airbag characteristics varied. Concerning the airbag, the mass and the initial velocity of the airbag support varied.

*Criterion determination*

The first step towards determining the new criterion was to calculate the maximal thoracic deflection due to the belt. This was made possible by using the shoulder belt force, once the mechanical behavior of the chest was determined. The thoracic deflection was measured at five points on the thorax: at the central point, at upper right and left points and at lower right and left points. The maximal deflection among the five points was found at the central point of the thorax for the simulations with belt-only restraint.

Several relationships between the shoulder belt load and the maximal deflection, corresponding to the central deflection, for a shoulder belt restraint were envisaged. For each relationship, the coefficients, which best model the relationship, were determined for each of the 35 simulations with a shoulder belt restraint. The mean and the standard deviation of these coefficients were calculated for each relationship. The best relationship was obtained with linear stiffness and linear damping for the loading and the unloading phases, as described in Equation 1. The maximal deflection was then calculated by resolving the differential Equation 1 with a Runge-Kutta method.

As presented in TableA 1, the shoulder belt configurations varied concerning the shoulder belt load limiter, the shoulder belt anchorage, the knee bolsters characteristics, the deceleration pulse, the initial velocity and the crash angle. Despite these differences of configuration and the number of simulations, the best k and c coefficients for the modeling of each shoulder belt load/maximal deflection relation presented means of k= 98N/mm and c= 0.4 N.s/mm with low standard deviations of 7 N/mm and 0.2 N.s/mm. These k and c values were used to calculate the maximal deflection caused by the belt from the shoulder belt load measurement, whatever the restraint system considered.

In the case of the shoulder belt restraint, it was verified whether or not the calculated maximal localized deflection corresponded to the sternal deflection (Figure 5). Despite a reasonably good correlation coefficient, quite a wide spread of measured deflection can be observed for the same calculated deflection. This will be discussed farther in the article.

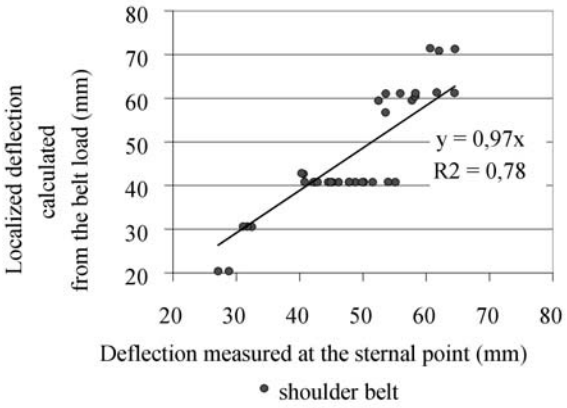


**Figure 5: Comparison of the maximal deflection measured and of the maximal deflection calculated from the belt load for the human body model**

The second step of the criterion determination was to calculate the maximal thoracic deflection due to the airbag using the Equation 2.

In the case of the airbag restraint, there is no shoulder belt load and, therefore, no localized deflection. The distributed deflection therefore equals the sternal deflection.

The last step of the criterion determination was to calculate the equivalent deflection based on the separate deflections due to the shoulder belt and the airbag using the Equation 3.

In order to determine the normalization factor, the risk curves as a function of the calculated localized deflection for the shoulder belt restraint and as a function of the calculated distributed deflection for the airbag restraint were used (Figure 6).

The slopes of the two risk curves were not identical. This could be due to the fact the calculated sternal deflection is not totally appropriate for predicting the thoracic risk for a given loading configuration, even if it is the main explanatory factor of the risk for a loading configuration. A way to minimize the error concerning the factor value was to calculate the normalization factor values for each level of risk and to use the mean of these values as the normalization factor. This corresponds to the calculation of the normalization factor value at 50% risk. At 50% risk, the localized deflection was 41 mm and the distributed deflection was 72 mm which resulted in a normalization factor of 0.57.

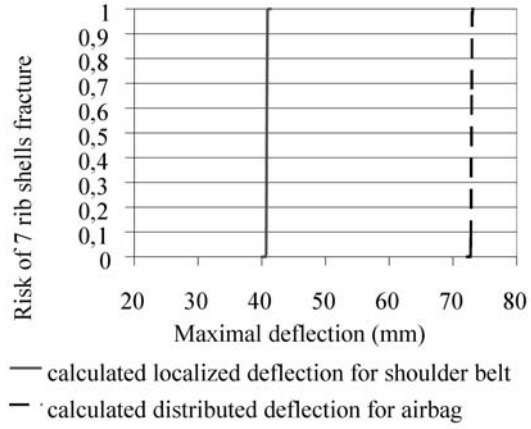


**Figure 6: Human body model risk curve as a function of the maximal localized and distributed deflections for the normalization factor calculation**

**Hybrid III/PMHS**

*Test configuration*

As with the human body model, test configurations with various restraints were needed for the evaluation of thoracic criteria. A part of the database of Hybrid III and PMHS tests presented by Kent et al. (2001) was used to validate the new criterion. It was a sorted sample taken from sled test data base presented by Kuppa and Eppinger (1998), excluding tests in which the PMHS or dummy head struck the windshield or in which there were large differences between the kinematics of the PMHS and the dummy. Additional Hybrid III and PMHS sled tests presented by Petitjean et al. (2002) were added. For each crash configuration, at least one Hybrid III and one PMHS test were performed in a crash test configuration with identical buck, deceleration pulse, and restraint condition.

Some of the data presented by Kent et al. were not available. The final analysis included 32 Hybrid III tests and 48 PMHS tests. Injuries of each PMHS were associated to dummy measurements in order to construct the risk curve as a function of dummy criteria. When there were several Hybrid III tests corresponding to PMHS tests for a given crash configuration, the mean of the dummy measurements was associated with each PMHS injury. This yielded 48 Hybrid III/PMHS test pairs (TableA 4, TableA 5, TableA 6, TableA 7 in appendix).

The distribution of low and high injury level cases of the final data sample was considered with respect to the restraint system (Figure 7) and to sled velocity (Figure 8). The choice of 6 rib fractures as a threshold is justified further on in this article.

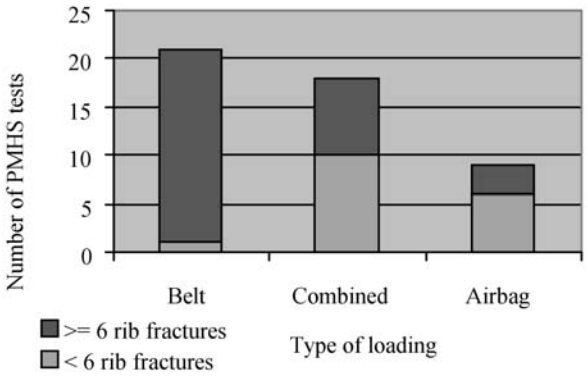


**Figure 7: Number of tests based on the rib fracture number, according to the restraint system**

Most of the belt restraint tests resulted in injury levels higher than the threshold of 6 rib fractures while most of the airbag restraint tests resulted in injury levels lower than to 6 rib fractures. The type of restraint was therefore considered to be contributing factor in the determination of risk for the analysis sample.

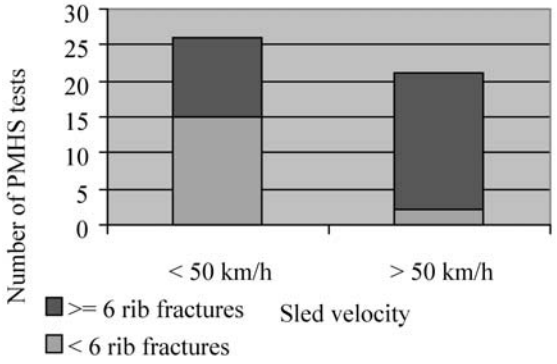


**Figure 8: Number of tests based on the rib fracture number, according to the sled initial velocity**

The sled velocity was also an influencing factor on the risk, given the much greater proportion of tests yielding injury levels higher than 6 rib fractures for sled velocity over 50 km/h compared to that of sled velocities under 50 km/h.

*Effect of PMHS characteristics on injury*

The PMHSs considered differed in their mass, age and gender. It was necessary to determine whether these characteristics were a major influence on the injury tolerance.

The distribution of low and high injury level cases of the final data sample was considered with respect to the PMHS age (Figure 9), PMHS gender (Figure 10), of PMHS weight (Figure 11), restraint system and PMHS age (Figure 12).

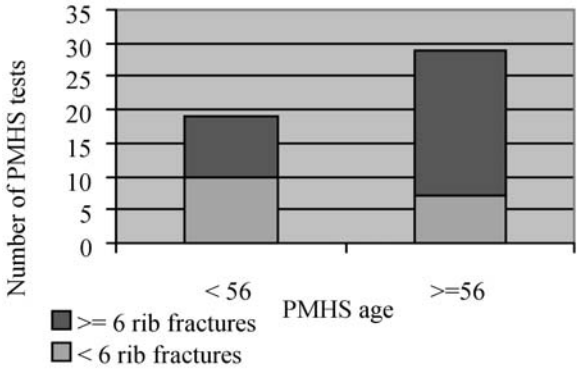


**Figure 9: Number of tests based on the rib fracture number, according to the PMHS age**

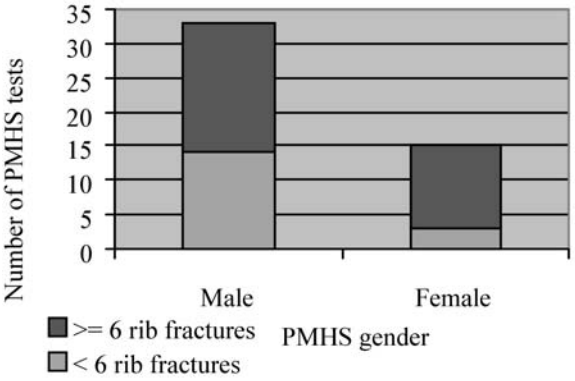


**Figure 10: Number of tests based on the rib fracture number, according to the PMHS gender**

As indicated in Figure 9, the proportion of PMHS tests resulting in injury levels higher than 6 rib fractures is greater over the mean age of the analysis sample (56-year-old) than it is under the mean age (75% compared to 47%). Age appears, therefore, to be a factor influencing the injury risk. Moreover, as indicated in Figure 10, the proportion of female PMHS tests yielding injury levels higher than 6 rib fractures was greater than the proportion of male PMHS tests (80% compared to 58%). This suggests that PMHS gender may also be a factor in determining injury risk. As indicated in Figure 11, the proportion of PMHS tests yielding injury levels higher than 6 rib fractures was similar above and below the mean mass of the analysis sample (70 kg). This indicates that PMHS mass may not be an influencing factor.

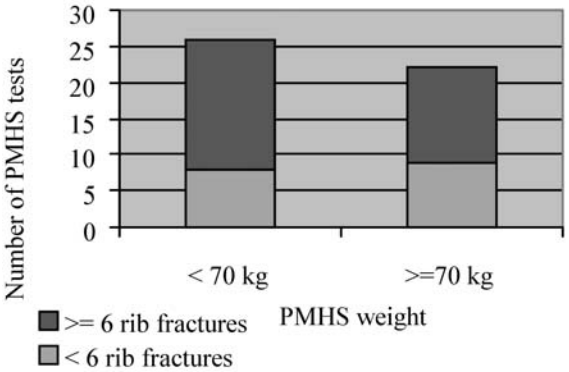


**Figure 11: Number of tests based on the rib fracture number, according to the PMHS mass (the mass for the test 357 and 358 was not available)**

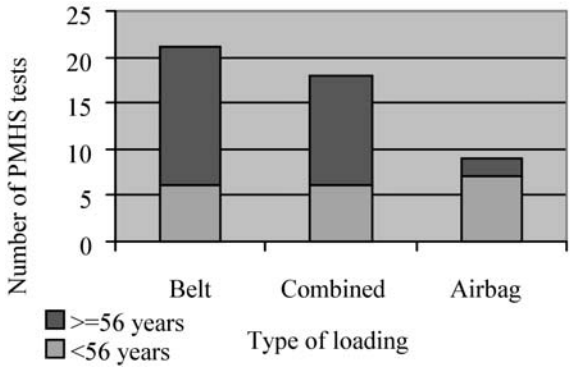


**Figure 12: Number of tests based on PMHS age, according to the restraint system**

In order to quantify the influence of the PMHS characteristics, risk curves were constructed, using the certainty method, for each characteristic. The statistic c index was calculated for each risk curve. The index values were 0.66 for age, 0.67 for gender, 0.52 for mass and 0.55 for height . This means that PMHS age and gender were influencing explanatory factors of the injury tolerance.

In this case, the influence of PMHS gender on the injury risk may result from the lack of female PMHSs, particularly yielding fewer than 6 rib fractures. Moreover, the mean age of female PMHSs is 61.7 +/-10.2 years whereas the mean age of male PMHSs is 53.2 +/-14 years. As PMHS age is an influencing factor determining injury tolerance, this may explain why the gender was also found to be an influencing factor, even if the age difference is not significant. Moreover, no clear influence of gender on the injury risk was determined in the literature ((Kent et al. (2001)). It was therefore decided that only PMHS age should be taken into account as an influencing PMHS factor.

As indicated in Figure 12, the proportion of PMHS of more than 56 years was similar for the belt and the combined restraint but was much lower for the airbag restraint. It was therefore necessary to take the PMHS age into account in order to correct the bias due to the sample repartition.

Concerning the influence of the PMHS age on the injury risk, Zhou et al. (1996) determined a correction of 0.33 rib fracture per year based on the time of death (correlation coefficient 0.78) from 107 shoulder belt restraint tests performed by Eppinger et al (1976). They suggested that the correction of the tolerance criterion with age is lower with blunt loading compared to belt loading. However, they also noticed that the lack of young PMHSs in the sample analysis under blunt loading could have underestimated the tolerance level of the young group and could have lowered the tolerance reduction with age. Moreover, Zhou et al. found the deflection rates under blunt loading to be 5 times higher than under airbag loading (Yoganadan et al. (1993), Kroell et al. (1971, 1974)) whereas the deflection rates are within the same range under shoulder belt and airbag loading. Therefore, as the deflection rates are similar under shoulder belt and airbag loading, it is supposed that the contribution level of the ribcage and the internal organs in the injury tolerance is also similar. It is not possible to verify that the deflection rates were similar for the PMHSs included in the analysis sample because the deflection measurements were not available. For information, it was verified for the Hybrid III included in the whole sample data (2.1+/-0.7 m/s for the shoulder belt; 1.5+/-0.5 m/s for the combined restraint; 1.9+/-1.5 m/s for the airbag loading). The reduction of tolerance with age was considered similar for the shoulder belt and airbag loading. Therefore, the correction of 0.33 rib fractures per year was applied for the whole analysis sample using the number of rib fractures and the PMHS age at the time of death.

*Criterion determination*

Before calculating the equivalent deflection, two physical parameters have to be determined: the maximal deflection due to the belt and the maximal deflection due to the airbag. In the case of the Hybrid III, and contrarily to the human body model, the sum of these two deflections is not necessarily equal to the central deflection measured by the rod potentiometer sensor. Indeed, if the rod potentiometer sensor is likely to measure the maximal deflection when loaded by an airbag, it is not the case when loaded by a belt, because of its sensitivity to the belt path. As a consequence, two different methods will be used to determine, in the one hand the maximal deflection related to the airbag and in the other hand the maximal deflection related to the belt.

Maximal deflection related to the airbag (indice 1 of flow chart in appendix C) - In the case of an airbag restraint, as the loading area on the thorax is very large, it is supposed that the deflection is similar under the whole contact area. The central deflection therefore represents correctly the maximal deflection due to the airbag.

In the case of a combined restraint, the maximal distributed deflection will be accurately estimated at the central point if the localized deflection at the central point is also accurately calculated, as shown by the Equation 2 (indice 3 of flow chart in appendix C), where $d_d$ (t) is the central distributed deflection,

$d_t(t)$ is the central deflection measured with the rod potentiometer (standard Hybrid III sternal displacement measurement transducer), $d_l$ (t) is the central localized deflection calculated.

The error in the calculation of the localized deflection at the central point is minimized if the stiffness calculated at this point is close to the real central stiffness.

The relationship between the shoulder belt load and the central deflection for a belt restraint was found to be as Equation 1.

The process to determine and optimize k and c of this Equation 1 is described in appendix B. This process consisted in defining initial values for k and c and then to correct them in order to address inconsistencies in results (indice 1b of flow chart in appendix C).

Maximal deflection related to the belt (indice 2 of flow chart in appendix C) – The maximal deflection on the thorax is supposed to be located under the loading area. In the case of a belt restraint, the loading area is limited to the contact area between the belt and the thorax. The central deflection will therefore correspond to the maximal deflection on the thorax only if the belt path passes over the central deflection sensor. When the belt path passes elsewhere, the central deflection sensor measures a smaller deflection. Moreover, it is supposed that the maximal belt load is poorly influenced by the belt path on the thorax. As a consequence, when the central deflection corresponds to the maximal deflection on the whole thorax, the stiffness calculated with the central deflection is minimal ($k = F_{belt}/d_{l\,max}$). This means the minimum stiffness calculated with the central deflection links the belt load at the time of maximal deflection to the maximal deflection in the particular case for which the belt path passes on the central deflection sensor. It is supposed that the relationship between the belt load at the time of maximal deflection and the maximal localized deflection on the whole thorax is identical, whatever the belt path. The minimum stiffness calculated with the central deflection, named $k_l$, will therefore be used to calculate the maximal deflection due to the belt on the whole thorax using the belt load, independently of the belt path.

$k_l$ was determined using Hybrid III belt-only tests data. The path of the shoulder belt on the thorax with respect to the central deflection sensor was not known. As a consequence, it was not possible to select belt-only tests for which the belt path was known to be on the central deflection sensor in order to calculate the $k_l$ stiffness. Therefore, the relationship between the belt load and the deflection (Equation 1) was first calculated for each belt-only test. Secondly, the minimum stiffness among all the belt-only tests was estimated.

The two points presenting the smallest stiffness for each level of belt load were considered and the minimum stiffness calculated using these points with the central deflection is described in Equation 4.

$$k_l = -0.0109 * F_{belt\,max} + 265 \qquad \text{(Equation 4)}$$

with $k_l$ in N/mm and $F_{belt}$ in N, $R^2$=0.4.

Equivalent deflection calculation - After having determined the maximal localized and distributed deflections on the thorax, the last stage in determining the criterion is to calculate the equivalent deflection based on these separate deflections and therefore to calculate the normalization factor. The normalization factor was calculated with risk curves for a level of risk similar to the one of the final risk curve.

The final risk curve was chosen to be constructed at the level of AIS3+ risk, in order to compare the final risk curve as a function of the equivalent deflection with the accidentological results. The number of rib fractures corresponding to AIS3+ has to be determined. The relationship was established by superimposing two shoulder belt load injury risk curves. One of these was proposed by Foret-Bruno et al. (1998) using accidentological data for AIS3+ risk, and the other constructed using PMHS data for a given number of rib fractures. The number of rib fractures which allows to superimpose both risk curves is considered to correspond to an accidentological AIS3+. The risk curve using PMHS data was constructed from the data set of PMHS tests performed by the APR (Peugeot Renault Association) between 1973 and 1988, which contains various configurations of frontal impact with three-point belt-only restraint. The sample consisted of 51 tests. Configuration details and PMHS characteristics are presented in TableA 10. A number of rib fractures equal to or higher than 6 was found to correspond to an accidentological AIS3+.

Normalization factor calculation - The risk curves used to calculate the normalization factor were then constructed with this threshold of 6 rib fractures. The analysis sample was not used for the determination of the normalization factor because the airbag restraint tests do not allow the construction of risk curve. Other data should be used.

In order to determine the normalization factor, two risk curves were used. One curve was constructed from belt-restrained PMHS data plotted against maximal localized deflection; the other from PMHS impactor test data plotted against maximal distributed deflection.

The first curve was constructed with the APR belt test data. The risk curve was first constructed with respect to the maximal shoulder belt load normalized for 78 kg using the procedures proposed by Eppinger et al. (1984). Indeed, the PMHS mass was found to be an influencing factor on the injury risk. It was necessary to construct the risk curve with respect to the maximal localized deflection using the APR sample based on the maximal shoulder belt load. The Equation 1 was then considered at the time when the localized deflection is maximal with the stiffness coefficient determined by Equation 4 and becomes:

$F_{belt\ d\ l\ max} = k_l\ d_{l\ max}$ , where $F_{belt\ d\ l\ max}$ is the belt load at the time when the localized deflection is maximal.

The relationship between the belt load at the time when the localized deflection is maximal and the maximal belt load was established using the 18 Hybrid III tests with belt-only restraint (Figure 13).

This shows that the maximal belt load was greater than the belt load at the time of maximal deflection as shown in Equation 5.

$$F_{belt\ d\ l\ max} = 0.844 * F_{belt\ max} \quad \text{(Equation 5)}$$

Equation 6 was determined using the Equation 1 at the time when the localized deflection is maximal and Equation 5.

$$F_{belt\ max} = (k_l/0.844)\ d_{l\ max} \quad \text{(Equation 6)}$$

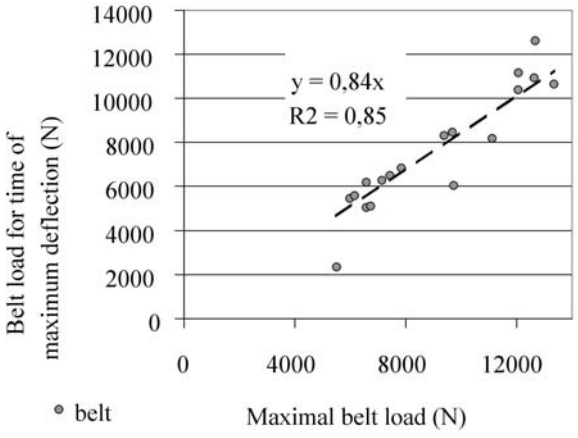


**Figure 13: Comparison of the maximal belt load and of the belt load at the time of maximal deflection**

The maximal shoulder belt loads from PMHS tests were then converted to dummy maximal localized deflection using Equation 6. Once the maximal shoulder belt load is converted to maximal localized deflection, a certainty method and logistic fitting of the results were performed in order to obtain the risk curve with respect to the maximal localized deflection.

The second curve was constructed from a data set of PMHS tests performed by Kroell et al. (1971, 1974) which consist of 35 impactor tests. The list of tests used is presented in TableA 11 in appendix. A risk curve constructed from airbag loading would have been preferred, but as too little data with Hybrid III exists and as the relationship between PMHS and Hybrid III deflection is not established for airbag loading, the risk curve from impactor tests was chosen as an initial approach.

The risk curve was first constructed as a function of the PMHS chest compression. It was necessary to construct the risk curve with respect to dummy maximal distributed deflection using the risk curve with respect to the PMHS compression. As proposed by Mertz et al. (1997), the PMHS chest compression was multiplied by the chest depth of the 50$^{th}$ percentile Hybrid III dummy. 13 mm were subtracted from the chest deflection obtained in order to take into account the compression of the flesh covering the sternum. Once the PMHS chest compression is converted to maximal distributed deflection, a certainty method and logistic fitting of the results were performed in order to obtain the risk curve with respect to the maximal distributed deflection.

The rib fractures were corrected by 0.33 fracture per year for the belt restraint tests, as indicated above, using the number of rib fractures and the PMHS age at the time of death. Zhou et al. observed the tolerance reduction with age is nearly 4 times lower for the impactor loading compared to the shoulder belt loading. However, they noticed that the sample was not well distributed according to PMHS age and so the tolerance reduction according to age could have been underestimated, as explained above. Therefore, the correction of rib fractures according to age should be between 0.1 and 0.33 rib fracture per year, which is the correction used for the shoulder belt restraint. Both rib fracture corrections were tested for the impactor tests, using the number of rib fractures and the PMHS age at the time of death.

Both risk curves must be constructed for the same age. Both samples contained a limited number of tests (51 and 35 tests). This may lead to erroneous

risk curves for some of the ages. The more information about injury risk that is exploited from the samples, the more accurate will be the risk curves for these given samples. The maximal amount of information is used from each sample when the number of points between the last point, with 0% risk, and the first point, with 100% risk, that is the number of points which contribute to the slope, is maximal. Moreover, the sample data is censored. The error due to the censoring is minimized when the proportion of right and left censored data that contribute to defining the slope is balanced.

The age for which the maximal number of tests contribute to defining the risk curve with respect to the localized deflection (82%) and for which the proportion of right and left censored is most balanced (55% left censored) is 40 years. As both risk curves must be constructed for the same age, it is necessary to verify that the information contained in the impactor test sample is sufficiently exploited for the age of 40-year-old. For 40-year-old and an injury correction of 0.33 fracture per year using the PMHS age at the time of death, the risk curve with respect to distributed deflection is defined by 80% of its number of tests and the proportion of right and left censored is balanced (39% left-censored). For 40-year-old and an injury correction of 0.1 fracture per year, the risk curve with respect to distributed deflection is defined by 80% of its number of tests and the proportion of right and left censored is balanced (46% left-censored). In conclusion, the information contained in both samples is best exploited for age 40. The risk curves constructed for this age are considered to be significant.

The risk curves which allow the determination of the normalization factor were then constructed with a threshold of 6 rib fractures and for 40-year-old. As for the human body model, the slopes of both risk curves were not identical. The normalization factor was determined for 50% risk. At 50% risk and 40-year-old, the maximal localized deflection is 33 mm and the maximal distributed deflection is between 75 mm (for rib fracture correction of 0.1) and 83 mm (for rib fracture correction of 0.33). The normalization factor is therefore between 0.40 and 0.44. As these two normalization factors are similar, the mean normalization factor of 0.42 was chosen to calculate the equivalent deflection. This normalization factor was determined for an age of 40 years in order to minimize the error due to the limited size of the samples used in the construction of the risk curves. However, without additional data, this normalization factor has to be considered as valid for all ages.

## RESULTS

### Validation of the equivalent deflection criterion

The principle of different contributions to the thoracic risk from the maximal localized and the distributed deflections had to be validated. In particular, the hypothesis of the calculation of the equivalent deflection as a resultant of the maximal localized and normalized distributed deflection should be confirmed. The hypothesis is shown to be valid if the risk curve for the combined belt and airbag restraint is similar to the risk curves for the belt-only and airbag-only restraints. The risk curves for the belt-only and airbag-only restraints are imperatively similar because of the normalization factor. Superimposing the risk curve for the combined restraint would confirm that the contribution of the belt and that of the airbag are taken sufficiently into account in the final risk. A single risk curve would therefore allow prediction of the risk for all the restraints.

Moreover, a c statistic value characterizing the risk curve as a function of the equivalent deflection, higher than the value characterizing the risk curve as a function of the existing criteria for the whole analysis sample would indicate that the equivalent deflection criterion is a better risk predictor than the existing criteria.

Lastly, accidentological results indicated that the injury risk is lower for the 4 kN load limiting belt plus airbag restraint than the risk associated with the 6 kN load limiting belt restraint. The efficiency of the combined restraint is not illustrated by the rod potentiometer deflection criterion (Petitjean et al. (2002)). If the equivalent deflection criterion was shown to reflect this difference in effectiveness, it would further indicate that the new criterion is a better predictor of the thoracic risk.

### Human Body Model

The appropriateness of the existing criteria for the prediction of thoracic risk is evaluated by constructing a risk curve with certainty method and calculating the statistic c value. The risk predicted by the sternal deflection is presented in Figure 14.

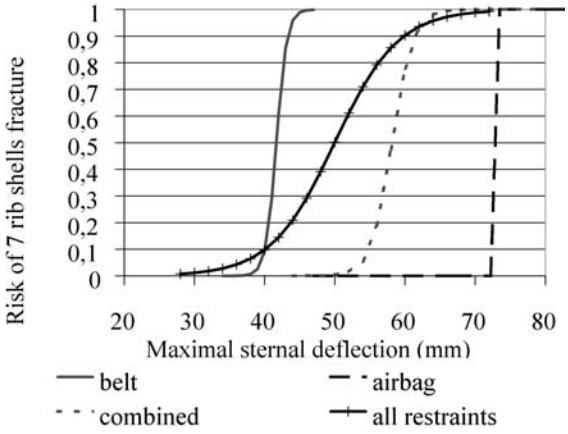


**Figure 14: Human body model risk curve as a function of the maximal sternal deflection**

The c statistic value for the risk curve including all restraints is 0.74. It is noticeable that the c statistic values for the risk curves for each restraint exceed 0.9. This shows that the sternal deflection criterion is a more appropriate risk predictor when only a single restraint type is considered, than when different restraints are compared.

The risk predicted by the viscous criterion is presented in Figure 15.

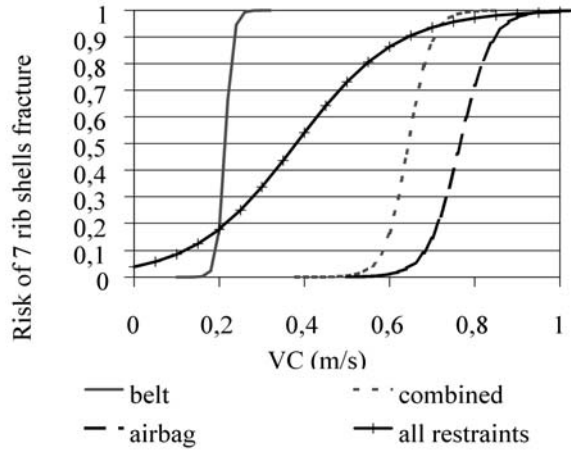


**Figure 15: Human body model risk curve as a function of the viscous criterion**

The c statistic value for the risk curve including all restraints is 0.55. It is noticeable the c statistic values for the risk curves for each separate restraint exceed 0.9. This shows that the viscous criterion is a more appropriate risk predictor when only a single restraint type is considered, than when different restraints are compared.

The risk predicted by the combined thoracic injury criterion is presented in Figure 16.

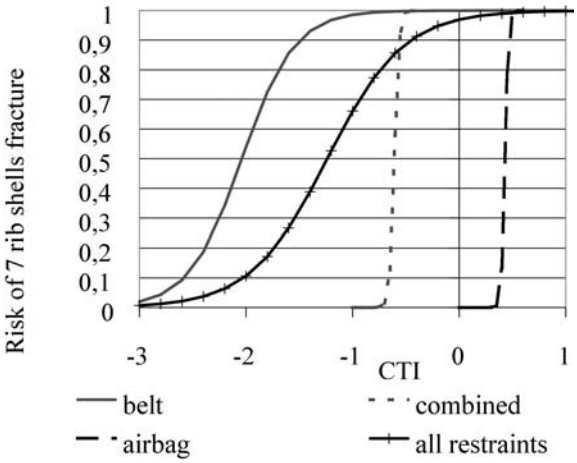


**Figure 16: Human body model risk curve as a function of the combined thoracic injury (CTI) criterion**

The c statistic value for the risk curve including all restraints is 0.79. It is noticeable the c statistic values for the risk curves for each separate restraint exceed 0.9. This shows that the CTI criterion is a more appropriate risk predictor when only a single restraint type is considered, than when different restraints are compared.

The risk predicted by the equivalent deflection criterion is now evaluated. The principle of the described equivalent deflection criterion will be validated if the risk curve as a function of the belt-only and airbag-only criterion is similar to the risk curve as a function of the combined restraint criterion, as explained above. These curves are presented in Figure 17.

The similitude of the above curves shows that the principle of the equivalent deflection as the resultant of the localized and the normalized distributed deflection is valid. The risk predicted by the equivalent deflection criterion for all the restraints yields a c statistic value of 0.88. It is noticeable the c statistic values for the risk curves for each restraint considered separately are around 0.9, which is close to the value for the risk curve for all restraints. The equivalent deflection criterion is therefore appropriate to predict the thoracic risk for all the restraints, belt, airbag or combined restraint as well as for each restraint type separately.

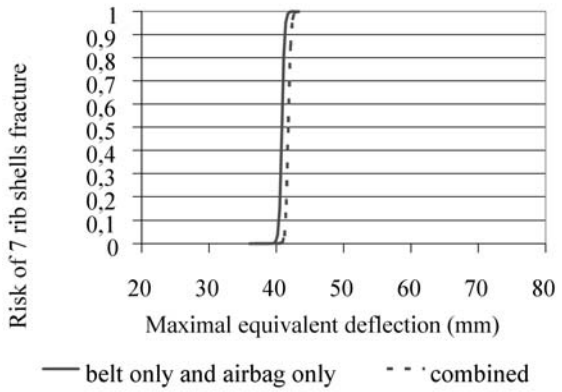


**Figure 17: Human body model risk curve as a function of the equivalent deflection criterion for the belt-only and airbag-only restraints compared to the combined restraint**

**Hybrid III/PMHS**

The analysis sample consists of limited tests number (48 tests). This may lead to erroneous risk curves for some of the ages. As explained above, the error due to the limited number of tests is minimized when the number of tests considered in constructing a curve is maximal and if the proportion of right and left censored tests considered is balanced.

The sternal deflection criterion is first evaluated. The age for which the most tests contribute to defining the risk curve as a function of the rod potentiometer deflection (81%) and for which the proportion of right and left censored among these tests is most balanced (49% left censored) is 50 years. The risk predicted by the sternal deflection for 50-year-old is presented in Figure 18.

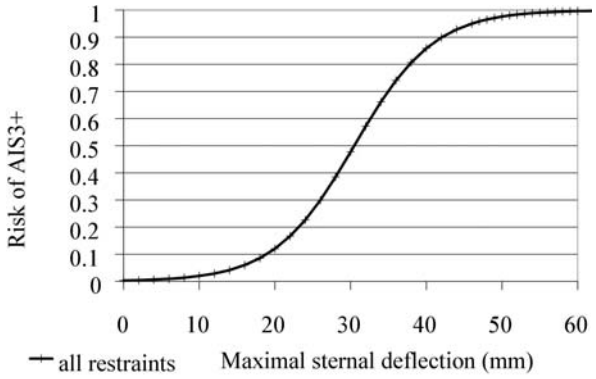


**Figure 18: Hybrid III risk curve as a function of the maximal sternal deflection for all restraints at 50-year-old**

The c statistic value for the risk curve including all restraints is 0.72.

The evaluation of the viscous criterion also requires the determination of the age for which the risk curve will be significant. The age for which the most tests contribute to defining the risk curve as a function of the viscous criterion (81%) and for which the proportion of right and left censored among these tests is most balanced (49% left censored) is 50 years. The risk predicted by the viscous criterion for 50-year-old is presented in Figure 19.

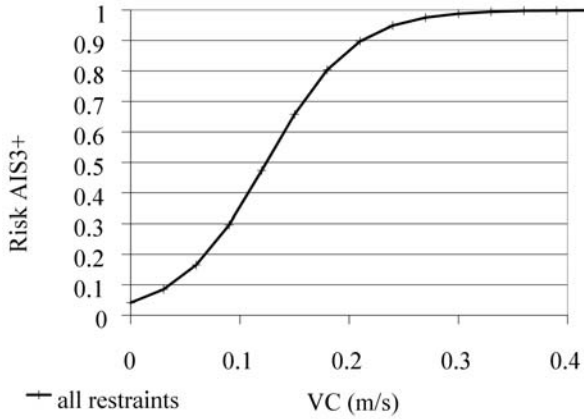


**Figure 19: Hybrid III risk curve as a function of the viscous criterion at 50-year-old**

The c statistic value for the risk curve including all restraints is 0.72.

Finally, the combined thoracic injury criterion is evaluated. The age for which the most tests contribute to defining the risk curve as a function of the CTI criterion (88%) and for which the proportion of right and left censored among these tests is most balanced (50% left censored) is 45 years. The risk predicted by the CTI for 45-year-old is presented in Figure 20.

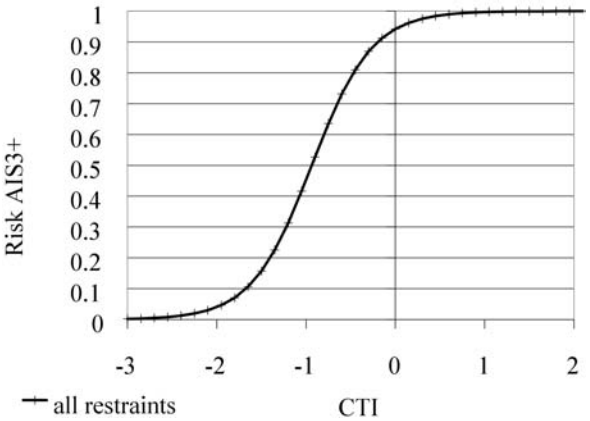


**Figure 20: Hybrid III risk curve as a function of the CTI criterion at 45-year-old**

The c statistic value for the risk curve including all restraints is 0.84.

It should be noted that the CTI criterion was calculated with the sternal deflection and not with the greatest deflection among several points on the thorax. The deflection was indeed measured only at one location on the Hybrid III thorax.

The risk predicted by the equivalent deflection is now evaluated. The first step of the evaluation of the equivalent deflection criterion is the validation of its principle. The principle of the equivalent deflection criterion as the resultant of the localized deflection and normalized deflection would be validated if the risk curve as a function of the criterion for the belt-only and airbag-only on one hand and for the combined restraint on the other hand superpose, as explained above.

The age for which the most tests contribute to defining the risk curve as a function of the equivalent deflection criterion (70% and 83%) and for which the proportion of right and left censored among these tests is most balanced (67% and 27% left censored) is 50 years. The risk curves as a function of the equivalent deflection for the belt-only and airbag-only restraints on one hand and for the belt and airbag combined restraint on the other hand are presented for 50-year-old in Figure 21.

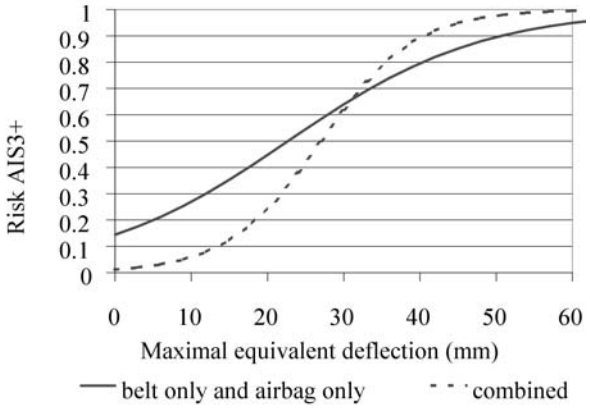


**Figure 21: Hybrid III risk curve as a function of the equivalent deflection criterion for the belt-only and airbag-only restraints compared to the combined restraint for 50-year-old**

The slopes of the two curves are not the same, so that they cannot coincide at all points. More, the belt-only and airbag-only curve is not consistent since there is a risk of 15% when there is no deflection. The differences may be due to the fact that the number of tests, the age, and the injury distribution differed in the two samples and that the one for belt-only and airbag-only is probably too small. This will be discussed later in the paper. The equivalent deflection for 50% of AIS3+ risk, however, is close for the two samples, 23 mm for the belt-only and airbag only restraints and 27 mm for the combined restraint. Therefore, in spite of the above reservations, the principle of the equivalent deflection as the resultant of the localized and the normalized distributed deflection is still considered valid at this point.

The risk predicted by the equivalent deflection criterion for all the restraints is constructed for age 45. Indeed, for this age, the maximal number of tests contributing to the slope (98%) and the most balanced proportion of right and left censored among these tests (51% left censored) were determined. The c statistic value for the risk curve including all restraints is 0.79.

For the four criteria evaluated, the risk curves for each restraint cannot be compared to the risk curve for all restraints because the limited number of tests by type of restraint does not allow construction of significant risk curves.

The final risk curve as a function of the equivalent deflection can be compared to the accidentological risk curve that was presented by Foret-Bruno et al. (1998) as a function of the maximal belt load. It was necessary to construct the risk curve as a function of the maximal equivalent deflection using the accidentological sample based on the maximal shoulder belt load.

Equations 1 and 6 were considered as well as Equation 7.

$$d_{eq\,max} = d_{l\,max} \qquad \text{(Equation 7)}$$

Once the maximal shoulder belt load is converted to maximal equivalent deflection, a certainty method and logistic fitting of the results were then performed, as presented by Foret-Bruno et al. The risk curve obtained is determined by Equation 8.

$$\text{Risk AIS3+} = 1/(1+\exp(17.5-\text{age}/5.8- d_{eq\,max}/3.3)) \qquad \text{(Equation 8)}$$

The risk curves as a function of the maximum equivalent deflection for age 45 is presented in Figure 22.

The slopes of the two risk curves are not identical. This may be due to the small number of tests in the analysis (48) compared to the number of tests in the accidentological study (256). The maximal equivalent deflection for 50% AIS3+ risk is similar. Given this, the two samples are considered to represent an equivalent population. As the number of tests is greater in the accidentological study sample,

the accidentological risk curve is considered more accurate than the risk curve based on the analysis sample and so will be used to predict the thoracic risk. Applying this risk curve to the analysis sample, the statistic c value was still equal to 0.79. The use of this risk curve will allow prediction the thoracic risk according to age.

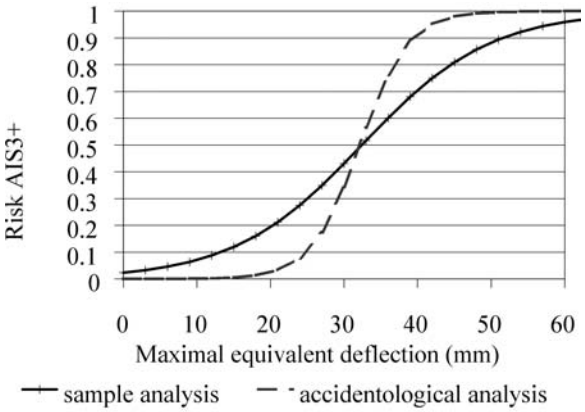


**Figure 22: Hybrid III risk curve as a function of the equivalent deflection criterion for sample analysis and the accidentological study for 45-year-old**

## DISCUSSION

The principle of the equivalent deflection criterion was validated using a human body model. Moreover, the c statistic values indicated that the equivalent deflection criterion is a better risk predictor (c=0.88) when considering all restraint types, than the sternal deflection criterion (c=0.74), the viscous criterion (c=0.55) and combined thoracic injury criterion (c=0.79). It should be noted that the existing criteria were found to be better risk predictor for a given restraint type than for all the restraints considered together. The equivalent deflection criterion, however, was found to be a better risk predictor considering all the restraint types as for a given restraint type.

Concerning the calculation of the maximal localized deflection, Figure 5 presented a large spread of measured deflections for the same calculated maximal localized deflection for belt-only restraints. This has to be explained by the variations in restraint geometry and crash conditions. While the restraint geometry and crash conditions vary, the shoulder belt force remains constant because of the load limiter. As the calculated maximal localized deflection is directly linked to the shoulder belt force, a given value of calculated maximal localized deflection globally corresponds to each limiting load, whatever the variations of crash configurations. On the contrary, the central deflection varies according to the crash configurations for a given load limiter. Therefore, several central deflections can correspond to a single maximal localized deflection calculated. If the central deflection is a better criterion than the shoulder belt force, then the equivalent deflection will be less efficient as a criterion for the belt-only restraint. However, one can observe this decrease of risk predictivity for the belt-only restraint, due to the spread of maximal localized deflections (up to 15 mm of central deflection for the same equivalent deflection) is highly compensated by the increase of the one for all restraint types due to the consideration of the different deflections tolerated for a same risk for a belt or an airbag. Indeed, for a given risk, the difference of central deflection between a belt and an airbag restraint can reach 30 mm. Finally, this demonstration is confirmed by the c coefficients, 0.88 for the equivalent deflection against 0.74 for the central deflection, for all restraint types.

Concerning the transfer of the criterion to the Hybrid III 50$^{th}$ percentile dummy, the maximal localized deflection was calculated from the belt load using the Equation 4, assuming that the relationship determined between the belt load and the central deflection, when the central deflection corresponds to the maximal deflection on the whole thorax (i. e. when the belt path is on the central deflection sensor), can be used to determine the maximal localized deflection from the belt load whatever the belt path.

Actually, the relationship between belt force and chest deflection is dependent on belt system geometry. It is not an invariant relationship for all belt systems, however, it has also not been quantified. Therefore, the degree to which it would alter the results of this work is unknown. This issue should be kept in mind when applying this method.

The measurement of the deflection among several points on the thorax would allow one to directly establish the relationship between the belt load and the maximal localized deflection whatever the belt path. It would result in a more accurate relationship than the one used in our analysis. However, this measurement was not available. Moreover, the error of the maximal localized deflection is lower considering the hypothesis described above than considering that the maximal localized deflection is equal to the central deflection whatever the belt path. As an example, several Hybrid III tests with belt restraint were performed with deflection measurements at five locations on the thorax (Petitjean et al. (2002)). The maximal localized deflection measured among five points on the thorax

was 31mm while the maximal central deflection measured was 19 mm and the calculation of the maximal localized deflection performed in our analysis gave 25 mm.

Similarly, the maximal distributed deflection was calculated from the belt load and the central deflection using the Equations 2 and B1 in appendix , as the maximal total deflection measurement is not available. The maximal shoulder belt load and the real stiffness are not highly correlated ($R^2$=0.3). This level of correlation means that some of the belt-only tests yielded a real stiffness higher or lower than the stiffness calculated with this equation. That is why it was necessary to evaluate the consequences on the criterion of using this relationship instead of a relationship which would precisely give the real central stiffness. The use of the real central stiffness in order to calculate the localized deflection would allow, in particular, the distributed deflection calculated to be zero in the case of a belt-only restraint.

For a real central stiffness higher than the one calculated, it was shown that the correction made for these tests allowed the corrected central stiffness to fit very closely the real central stiffness. For a real central stiffness lower than the calculated central stiffness, it was shown that the range of distributed deflection calculated was small for the belt-only tests and, in particular, lower than for the combined restraint tests. In conclusion, it was verified that the consequences on the equivalent deflection of the use of the Equation B1 in appendix, combined with the correction applicable instead of the real central stiffness, are limited enough to justify the use of the method.

The best solution would be to calculate the maximal distributed deflection at the thoracic point where the total deflection is maximal. In this case, the maximal distributed deflection would be correctly calculated using Equation 2.

As a result, the measurement of the maximal deflection on the thorax would allow :

- to determine a more confident relationship between the shoulder belt load and the maximal localized deflection for the belt-only tests,
- therefore to calculate the maximal localized and distributed deflections more precisely for combined restraint. In particular, it will prevent from finding a contribution of distributed deflection to the equivalent deflection in belt-only restaint test.

The measurement of the exact maximal deflection on the thorax would necessitate to measure the deflection at any thoracic point. As it is hardly feasible, the use of several deflection measurement points on the thorax is recommended in order to better estimate the total maximal deflection than the central deflection does.

Concerning the hypothesis of the calculation of the equivalent deflection as a resultant of the localized and the normalized distributed deflections, the risk curves with respect to the equivalent deflection for the belt-only and airbag-only restraints and for the combined restraint do not exactly correspond at 50% AIS3+. As the equivalent deflection is balanced by the normalization factor, it depends on the ratio between the distributed and the localized loading. A better definition of the injury risk curve for distributed loading (airbag instead of impactor) would probably improve the accuracy of this criterion and therefore allow the risk curves for the belt-only and airbag only restraints and for the combined restraint to fit more closely at 50% AIS3+.

Moreover, the c statistic value is slightly higher for the equivalent deflection (0.79) than for the sternal deflection criterion (0.72). The distribution of the analysis sample based on the restraint type may explain the relatively small improvement in risk prediction given by the equivalent deflection compared to the sternal deflection. In the analysis sample, the number of airbag restraint tests is much lower than the number of belt restraint tests. As the sternal deflection criterion gives two different limits for a given risk for belt and airbag loading, the lack of airbag restraint tests compared to number of the belt restraint tests tends to increase the c statistic value. On the other hand, as the equivalent deflection criterion aims to take into account different contributions to the risk for these two loading types in order to use a single limit, the lack of airbag restraint tests compared to the number of belt restraint tests tends to lower the c statistic value. One can suppose that a sample of well distributed data based on a given risk according to the different restraints would indicate a better appropriateness of the equivalent deflection for prediction of thoracic risk.

The c statistic value is slightly lower for the equivalent deflection (0.79) than for the combined thoracic injury criterion (0.84). The CTI criterion, however, is dependent on possible head impact on

car components (Petitjean et al (2002)) and therefore should not be applied without verifying the dummy kinematics.

Lastly, the equivalent deflection criterion illustrated the efficiency of a 4 kN load limiting belt and airbag restraint compared to a 6 kN load limiting belt restraint. For an age of 45 years, the equivalent deflection criterion indicated by the analysis sample is 15% for the combined restraint and 47% for the belt-only restraint. On the contrary, the sternal deflection criterion did not illustrate the efficiency of the combined restraint. For an age of 45 years, if referring to the analysis sample, the sternal deflection indicated a risk of 27% for the combined restraint and 13% for the shoulder belt restraint.

The risk curves with respect to the equivalent deflection determined, on the one hand with the analysis sample and, on the other hand with the accidentological study sample, were found to be similar at 50% risk AIS3+. The risks predicted by the equivalent deflection criterion based on accidentological data is given by the Equation 8.

The risk predicted by the shoulder belt load based on accidentological data (Foret-Bruno et al. (1998)) is given by the Equation 9.

$$\text{Risk AIS3+} = 1/(1+\exp(19.9-\text{age}/5.9-F_{beltmax}/557)) \quad \text{(Equation 9)}$$

Table 2 shows that the equivalent deflection criterion allows prediction of thoracic risk comparable to those predicted by the accidentological study.

**Table 2: Comparison of the thoracic risks predicted by the equivalent deflection criterion and by the shoulder belt load for the accidentological sample**

| | Equivalent deflection | | Shoulder belt load | |
|---|---|---|---|---|
| | 4 kN | 6 kN | 4 kN | 6 kN |
| 45 years | 0.01 | 0.11 | 0.01 | 0.18 |
| 60 years | 0.07 | 0.63 | 0.07 | 0.74 |
| 75 years | 0.51 | 0.96 | 0.50 | 0.97 |

The reader should note that the equivalent deflection criterion was found to be appropriate to predict thoracic risk for in-position occupants restrained by current restraints (belt, airbag or combined restraint). The pertinence of this criterion was not studied for other crash configurations (for example, out-of-position).

## CONCLUSION

The sternal deflection criterion gives two different tolerance limits according to whether loading is localized or distributed. None of these two criterion limits can be applied to a combined loading configuration. The equivalent deflection criterion described takes into account the different contributions to the risk of localized and distributed loads in a single criterion giving a single tolerance limit for all restraint types.

A numerical human body model was used in order to develop and validate the principle of the equivalent deflection criterion. It confirmed that the equivalent deflection criterion is more appropriate to predict thoracic risk for all restraint types than the sternal deflection criterion.

The criterion was then transferred to the Hybrid III dummy. The better efficiency observed in the accidentology study of a 4 kN load limiting belt and airbag restraint compared to a 6 kN load limiting belt was confirmed by the equivalent deflection criterion whereas it was not by the sternal deflection criterion. The final risk curve was issued from accidentological data.

The contribution of the maximal localized deflection is determined by a relationship with the shoulder belt load using central deflection data. This relationship did not show a high correlation. This may be due to the fact that the maximal localized deflection was not directly used to establish the relationship with the belt load. This also may be due to the influence of the belt system geometry which effect on the results is unknown. The use of the real maximal deflection on the thorax and the consideration of the belt restraint geometry may improve the reliability of the relationship between the belt load and the maximal localized deflection, and therefore that of the equivalent criterion.

The principle, validated by the simulations and transferred to the Hybrid III dummy has given very promising results. However, in order to totally validate the criterion, additional data is required. This is particularly true for airbag only loading configurations for which little data was available providing injured PMHS and Hybrid III measurements.

## ACKNOWLEDGMENTS

The authors would like to acknowledge NHTSA and the University of Virginia for providing time-history curves of their PMHS and Hybrid III data. They

would like also to acknowledge Martin Page for his English assistance in the writing of this article.

## REFERENCES

Besnault B., Lavaste F., Guillemot H., Robin S., Le Coz J.Y. (1998) A Parametric Finite Element Model of the Human Pelvis, Proceedings of the 42nd Stapp Car Crash Conference, Paper n° 983147, Society of Automotive Engineers, Warrendale, PA.

Crandall, J.R., Bass, C.R., Pilkey, W.D., Miller, H.J., Sikorski, J., Wilkins, M. (1996) An Evaluation of Thoracic Response and Injury with Belt, Airbag, and Force Limited Belt Restraint Systems, Proceedings of the NATO-ASI on Crashworthiness of Transportation Systems Structural Impact and Occupant Protection.

Eppinger, R.H. (1976) Prediction of Thoracic Injury using Measurable Experimental Parameters, 6th International Conferecne on Experimental Safety Vehicles, SAE-766073, pp770-780.

Eppinger, R.H., Marcus, J.H., Morgan, R.M. (1984) Development of Dummy and Injury Index for NHTSA's Thoracic Side Impact Protection Research Program. SAE Technical Paper 840885. Society of Automotive Engineers, Warrendale, PA.

Foret-Bruno, J-Y, Trosseille, X, Le Coz,, J-Y, Bendjellal, F, Steyer, C. (1998). Thoracic Injury Risk in Frontal Car Crashes with Occupant Restrained with Belt Load Limiter. SAE Paper No.983166, Proceedings of 42nd Stapp Car Crash Conference.

Horsch, J., Melvin, J.W., Viano, D.C., Mertz, H.J. (1991) Thoracic Injury Assessment of Belt Restraint Systems Based on Hybrid III Chest Compression. Proc. 35th Stapp Car Crash Conference, pp85-108. Society of Automotive Engineers, Warrendale, PA.

Kallieris, D., Stein, K.M., Mattern, R., Morgan, R., Eppinger, R. (1994) The Performance of Active and Passive Driver Restraint Systems in Simulated Frontal Collisions, Proc. 38th Stapp Car Crash Conference, pp165-175 Society of Automotive Engineers, Warrendale, PA.

Kallieris, D., Rizzetti, A., Wiren, B.V., Mattern, R. (1996) The Influence of Force Limiter to the Injury Severity by Using a 3-point Belt and Driver Airbag in Frontal Collisions, Paper n°96-S3-O-08, International Technical Conference on Experimental Safety Vehicles.

Kent, R., Bolton, J., Crandall, J., Prasad, P., Nusholtz, G., Mertz, H., Kallieris, D. (2001) Restrained Hybrid III Dummy-Based Criteria For Thoracic Hard-Tissue Injury Prediction, Proc. 2001 International IRCOBI Conference on the Biomechanics of Impact, pp215-232. IRCOBI, Bron, France.

Kroell, C.K., Schneider, D.C, Nahum, A.M. (1971) Impact Tolerance and Response of the Human Thorax. Proc. 15th Stapp Car Crash Conference, pp84-134. Society of Automotive Engineers, Warrendale, PA.

Kroell, C.K., Schneider, D.C, Nahum, A.M. (1974) Impact Tolerance and Response of the Human Thorax II. Proc. 18th Stapp Car Crash Conference, pp383-412. Society of Automotive Engineers, Warrendale, PA.

Kuppa, S., Eppinger, R.H. (1998) Development of an Improved Thoracic Injury Criterion. Proc. 42nd Stapp Car Crash Conference, pp139-154. Society of Automotive Engineers, Warrendale, PA.

Lau, I., Viano, D.C. (1986) The Viscous Criterion-Bases and Applications of an Injury Severity Index for Soft Tissue, Proc. 30th Stapp Car Crash Conference, p123-142. Society of Automotive Engineers, Warrendale, PA.

Lizee, E., Robin, S., Song, E., Bertholon, N., Le Coz, J-Y., Besnault, B., Lavaste, F. (1998) Development of a 3D Finite Element Model of the Human Body, Proc. 42nd Stapp Car Crash Conference, Paper n°983152, pp1-23. Society of Automotive Engineers, Warrendale, PA.

Mertz. H., Horsch, J., Horn, G., Lowne, R. (1991) Hybrid III Sternal Deflection Associated with Thoracic Injury Severities of Occupants Restrained with Force-Limiting Shoulder Belts. SAE N°910812, Society of Automotive Engineers International Congress and Exposition, Warrendale, PA.

Mertz, H., Prasad, P., Nusholtz, G. (1996) Head Injury Risk Assessment for Forehead Impacts , SAE paper N° 960099, International Congress and Exposition, Detroit, Michigan.

Mertz. H., Prasad, P., Irwin, A.L. (1997) Injury Risk Curves for Children and Adults in Frontal and Rear Collisions. Proc. 41st Stapp Car Crash Conference, pp13-30. Society of Automotive Engineers, Warrendale, PA.

Neathery, R.F., Kroell, C.K., Mertz, H.J. (1975). Prediction of Thoracic Injury from Dummy Responses, Proc. 19th Stapp Car Crash Conference, Paper n° 751151, Society of Automotive Engineers, Warrendale, PA.

Nusholtz, G., Mosier, R.(1999), Consistent Threshold Estimate for Doubly Censored Biomechanical Data, , Proc. 43rd Stapp Car Crash Conference, pp149-163 Society of Automotive Engineers, Warrendale, PA.

Petitjean, A., Lebarbe, M., Potier, P., Trosseille, X., Lassau, J-P. (2002) Laboratory Reconstructions of Real World Frontal Crash Configurations using the Hybrid III and THOR Dummies and PMHS, Stapp Car Crash Journal 46: 27-54.

Yoganadan, N., Skrade, D., Pintar, F.A., Reinartz, J., Sances, A. (1991) Thoracic Deformation Contours in a Frontal Impact. Proc 35th Stapp Car Crash Conference, pp. 47-63. Society of Automotive Engineers, Warrendale, PA.

Yoganandan, N., Pintar, F.A., Skrade, D., Cmiel, W., Reinartz, J.M., Sances Jr, A. (1993) Thoracic Biomechanics with Air Bag Restraint, Proc. 37th Stapp Car Crash Conference, p133-144. Society of Automotive Engineers, Warrendale, PA.

Zhou, Q., Rouhana, S.W., Melvin, J.W. (1996) Age Effects on Thoracic Injury Tolerance, Proc. 40th Stapp Car Crash Conference, Paper N°962421, p137-148. Society of Automotive Engineers, Warrendale, PA.

## APPENDIX A

**TableA 1: Description of the shoulder belt restraint simulations**

| Simulation number | Load limiter (N) | Vi (m/s) | Gamma (g) | Crash angle (°) | SB | KB |
|---|---|---|---|---|---|---|
| EH_CEI54 | 3000 | 8 | 10 | 0 | R1 | AG1 |
| EH_CEI64 | 3000 | 8 | 10 | 15 | R1 | AG1 |
| EH_CEI66 | 3000 | 8 | 10 | -15 | R1 | AG1 |
| EH_CEI68 | 4000 | 10 | 14 | 0 | R1 | AG1 |
| EH_CEI80 | 6000 | 6 | 7 | 0 | R1 | AG1 |
| EH_CEI82 | 2000 | 10 | 14 | 0 | R1 | AG1 |
| EH_CEI50 | 4000 | 10 | 12 | 0 | R1 | AG1 |
| EH_CEI30 | 4000 | 15.5 | 13 | 0 | R1 | AG1 |
| EH_CEI88 | 6000 | 6 | 11 | 0 | R1 | AG1 |
| EH_CEI72 | 4000 | 15.5 | 16 | 0 | R1 | AG1 |
| EH_CEI70 | 3000 | 15.5 | 16 | 0 | R1 | AG1 |
| EH_CEI60 | 4000 | 15.5 | 13 | 15 | R1 | AG1 |
| EH_CEI90 | 6000 | 8 | 15 | 0 | R1 | AG1 |
| EHCEI100 | 7000 | 8 | 15 | 0 | R1 | AG1 |
| EHCEI102 | 7000 | 6 | 11 | 0 | R1 | AG1 |
| EHCEI106 | 7000 | 10 | 14 | 0 | R1 | AG1 |
| EHCEI108 | 6000 | 10 | 10 | 0 | R1 | AG1 |
| EHCEI110 | 7000 | 10 | 10 | 0 | R1 | AG1 |
| EH_CEI58 | 4000 | 10 | 12 | 15 | R1 | AG1 |
| EH_CEI56 | 4000 | 10 | 12 | -15 | R1 | AG1 |
| EH_CEI78 | 6000 | 8 | 10 | 0 | R1 | AG1 |
| EH_CEI84 | 6000 | 10 | 19 | 0 | R1 | AG1 |
| EH_CEI94 | 7000 | 10 | 19 | 0 | R1 | AG1 |
| EH_CEI48 | 6000 | 15.5 | 16 | 0 | R1 | AG1 |
| EH_CEI44 | 6000 | 15.5 | 21 | 0 | R1 | AG1 |
| EH_CEI62 | 4000 | 15.5 | 13 | -15 | R1 | AG1 |
| EHCMXY72 | 4000 | 15.5 | 19 | 0 | R2 | AG1 |
| EHCMXZ72 | 4000 | 15.5 | 19 | 0 | R3 | AG1 |
| EHCPXY72 | 4000 | 15.5 | 19 | 0 | R4 | AG1 |
| EHCPXZ72 | 4000 | 15.5 | 19 | 0 | R5 | AG1 |
| EHGCEI68 | 4000 | 10 | 14 | 0 | R1 | None |
| EHGCEI72 | 4000 | 15.5 | 16 | 0 | R1 | None |
| EHGCEI80 | 6000 | 6 | 7 | 0 | R1 | None |
| EHGCEI82 | 2000 | 10 | 14 | 0 | R1 | None |
| EHHCEI72 | 4000 | 15.5 | 16 | 0 | R1 | AG2 |

**SB : Shoulder belt anchorage**
The origin of the skew is the middle point between the cotyles. The X axis is forward, the Z axis is upward. The different anchorages used in the simulations are:

R1 : X= 330 ; Y=250 ; Z=590
R2 : X=330 ; Y=210 ; Z=590
R3 : X=330 ; Y=250 ; Z=690
R4 : X=330 ; Y=300 ; Z=590
R5 : X=330 ; Y=250 ; Z=490

**KB : Knee Bolster type**
Several laws of material were tested in the simulations, as described by:

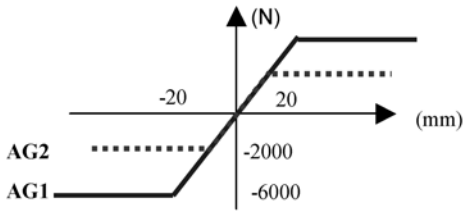

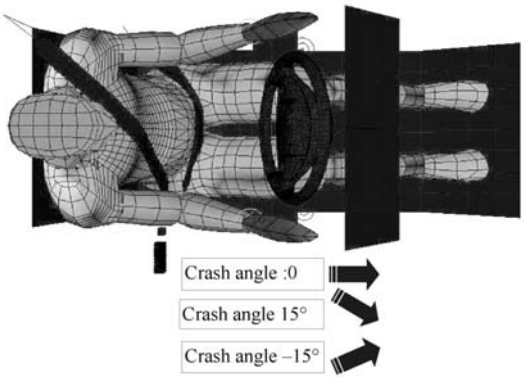


**FigureA 1: Upper view of the shoulder belt and shoulder belt and airbag restraint configurations**

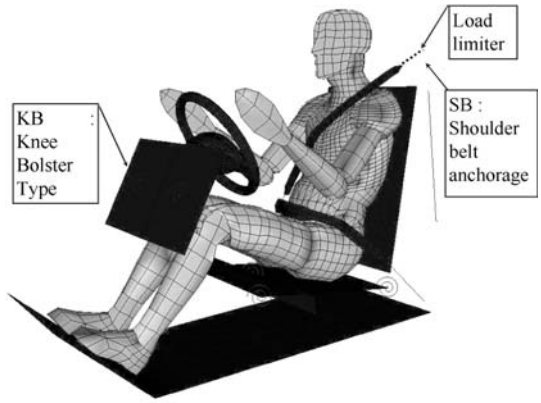


**FigureA 2: Lateral view of the shoulder belt and shoulder belt and airbag restraint configurations**

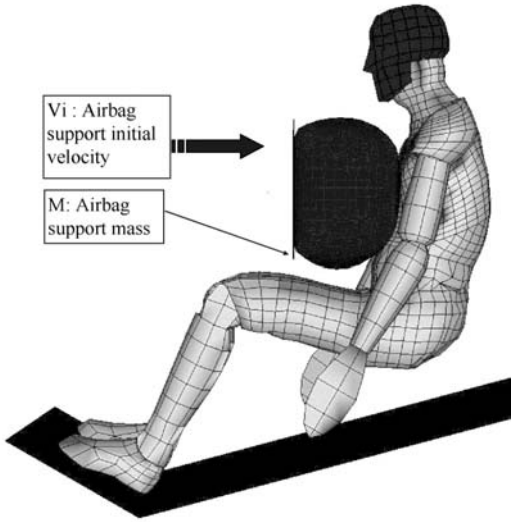


**FigureA 3: Lateral view of the airbag restraint configuration**

**TableA 2: Description of the shoulder belt and airbag restraint simulations**

| Simulation number | Load limiter (N) | Vi (m/s) | Gamma (g) | Crash angle (°) | SB | AB |
|---|---|---|---|---|---|---|
| EH_CEI37 | 3000 | 10 | 14 | 0 | R1 | AB1 |
| EH_CEI47 | 3000 | 10 | 14 | 15 | R1 | AB1 |
| EH_CEI49 | 3000 | 10 | 14 | -15 | R1 | AB1 |
| EH_CEI43 | 4000 | 10 | 19 | 15 | R1 | AB1 |
| EH_CEI35 | 4000 | 10 | 14 | 0 | R1 | AB1 |
| EH_CEI57 | 4000 | 10 | 14 | 0 | R1 | AB1 |
| EH_CEI59 | 2000 | 6 | 11 | 0 | R1 | AB1 |
| EH_CEI61 | 6000 | 6 | 7 | 0 | R1 | AB1 |
| EH_CEI65 | 3000 | 6 | 11 | 0 | R1 | AB1 |
| EH_CEI29 | 4000 | 10 | 19 | 0 | R1 | AB1 |
| EH_CEI45 | 4000 | 10 | 19 | -15 | R1 | AB1 |
| EH_CEI41 | 4000 | 15.5 | 16 | 0 | R1 | AB1 |
| EH_CEI17 | 4000 | 15.5 | 21 | 0 | R1 | AB1 |
| EHOCEI17 | 4000 | 15.5 | 21 | 0 | R1 | AB2 |
| EHOCEI35 | 4000 | 10 | 14 | 0 | R1 | AB2 |
| EHOCEI57 | 4000 | 10 | 14 | 0 | R1 | AB2 |
| EHQCEI17 | 4000 | 15.5 | 21 | 0 | R1 | AB3 |
| EHQCEI35 | 4000 | 10 | 14 | 0 | R1 | AB3 |

**AB : airbag type**
Several type of airbag were simulated:
AB1 : pressure venting =0.5 bar; venting surface =3200 mm2
AB2 : pressure venting =0.7 bar; venting surface =3200 mm2
AB3 : pressure venting =0.5 bar; venting surface =1600 mm2

**TableA 3: Description of the airbag restraint simulations**

| Simulation number | Load limiter (N) | Vi (m/s) | Gamma (g) | Crash angle (°) | AB |
|---|---|---|---|---|---|
| EH_SAT57 | / | 10 | 14 | 0 | AB7 |
| Simulation number | Airbag support mass (kg) | Airbag support Vi (m/s) | Gamma (g) | Crash angle (°) | |
| EH_SAC25 | 46.8 | 4 | / | 0 | AB8 |
| EH_SAC28 | 46.8 | 6 | / | 0 | AB8 |
| EH_SAC30 | 55 | 6 | / | 0 | AB8 |
| EH_SAC22 | 46.8 | 8 | / | 15 | AB8 |
| EH_SAC16 | 46.8 | 8 | / | 0 | AB8 |
| EH_SAC33 | 46.8 | 10 | / | 0 | AB8 |
| EH_SAC17 | 46.8 | 12 | / | 0 | AB8 |
| EH_SAC18 | 55 | 8 | / | 0 | AB8 |
| EH_SAC21 | 46.8 | 8 | / | 15 | AB8 |
| EH_SAC23 | 46.8 | 11.2 | / | 15 | AB8 |
| EH_SAC34 | 46.8 | 15 | / | 0 | AB8 |

**AB : airbag type**
AB7 : pressure venting =0.7 bar; venting surface =2000 mm2
AB8: impacting airbag fixed no venting on an airbag support

**TableA 4: UVA PMHS tests included in the analysis sample (Kent et al. (2001))**

| PMHS test number | HIII test number | Restraint type |
|---|---|---|
| 53 | 52 | Belt |
| 55 | 54 | Belt |
| 102 | 101 | Belt |
| 103 | | |
| 104 | | |
| 223 | 222 | Belt |
| 224 | | |
| 225 | | |
| 250 | 249 | Belt |
| 252 | 251 | Belt |
| 257 | 256 | Belt |
| 258 | | |
| 259 | | |
| 294 | 293 | Belt |
| 295 | | |
| 296 | | |
| 333 | 332 | Combined |
| 334 | | |
| 335 | | |
| 356 | 355 | Airbag |
| 357 | | |
| 358 | | |
| 533 | 537, 538 | Combined |
| 534 | | |
| 535 | | |
| 544 | | |
| 545 | | |
| 577 | 572, 576 | Combined |
| 578 | | |
| 579 | | |
| 580 | | |
| 650 | 648, 649 | Airbag |
| 651 | | |
| 652 | | |
| 665 | 663, 664 | Combined |
| 666 | | |
| 667 | | |
| 668 | | |

**TableA 5: Heidelberg PMHS tests included in the analysis sample (Kent et al. (2001))**

| PMHS test number | HIII test number | Restraint type |
|---|---|---|
| 9013 | 9002 | Belt |
| 9014 | 9003 | Airbag |
| 9207 | | |
| 9212 | | |

**TableA 6: PMHS tests included in the analysis sample (Yoganandan et al. (1991))**

| PMHS test number | HIII test number | Restraint type |
|---|---|---|
| MCW108 | 2780 | Belt |
| MCW110 | 2847 | Belt |

**TableA 7: CEESAR PMHS tests included in the analysis sample (Petitjean et al. (2002))**

| PMHS test number | HIII test number | Restraint type |
|---|---|---|
| C05 | C02, C03, C13, C18, C20 | Combined |
| C22 | | |
| C17 | C11, C12, C19, C21 | Belt |
| C23 | | |

**TableA 8: Hybrid III belt tests of the sample analysis used to determine the relation between the belt load and the sternal deflection**

| HIII test number | Maximal belt load (N) | Optimised stiffness (N/mm) | Optimised damping (N.s/mm) |
|---|---|---|---|
| 101 | 9380 | 116 | 2.2 |
| 108 | 7836 | 168 | 3.3 |
| 110 | 7428 | 174 | 3.1 |
| 222 | 11116 | 105 | 1.8 |
| 249 | 12053 | 147 | 2.1 |
| 251 | 13344 | 158 | 2.4 |
| 256 | 12632 | 165 | 2.5 |
| 293 | 9680 | 184 | 2.5 |
| 52 | 12060 | 178 | 2.5 |
| 54 | 12671 | 133 | 1.4 |
| 9002 | 9726 | 221 | 3.4 |
| Mean of C11. C12. C19. C21 | 6571 | 278 | 4.2 |

**TableA 9: Hybrid III belt tests out of the sample analysis used to determine the relation between the belt load and the sternal deflection**

| HIII test number | Maximal belt load (N) | Optimised stiffness (N/mm) | Optimised damping (N.s/mm) |
|---|---|---|---|
| 4827c | 5504 | 200 | 4.7 |
| 4827p | 5980 | 281 | 1.9 |
| 4863c | 6149 | 169 | 3 |
| 4848p | 6571 | 187 | 3.6 |
| 4877p | 6732 | 168 | 2.8 |
| 4875p | 7137 | 263 | 7.1 |

**TableA 10: APR PMHS tests**

| Test n° | PMHS age | PMHS mass | PMHS height | PMHS gender | Sled v | Sled deceleration | Max belt load | Rib fractures |
|---|---|---|---|---|---|---|---|---|
| / | year | kg | cm | | km/H | g | N | / |
| 3 | 57 | 70 | 170 | M | 48 | 13 | 4400 | 9 |
| 6 | 60 | 55 | 146 | F | 58 | 21 | 4900 | 18 |
| 25 | 66 | 55 | 166 | F | 50 | 13 | 4700 | 16 |
| 26 | 48 | 63 | 170 | M | 48 | 11 | 6300 | 11 |
| 27 | 53 | 70 | 175 | M | 50 | 12 | 5600 | 7 |
| 33 | 51 | 50 | 171 | M | 49 | 6 | 4200 | 2 |
| 34 | 58 | 61 | 164 | M | 49 | 10 | 5200 | 12 |
| 41 | 60 | 50 | 171 | M | 50 | 12 | 3700 | 1 |
| 53 | 46 | 63 | 165 | M | 36 | 5 | 4300 | 4 |
| 54 | 34 | 60 | 178 | M | 48 | 10 | 3700 | 0 |
| 115 | 52 | 63 | 155 | M | 50 | 12 | 6800 | 5 |
| 115 | 55 | 42 | 171 | F | 50 | 12 | 4800 | 0 |
| 117 | 60 | 53 | 163 | M | 50 | 19 | 5500 | 9 |
| 123 | 52 | 75 | 170 | M | 56 | 16 | 7600 | 10 |
| 127 | 43 | 42 | 159 | M | 50 | 14 | 4400 | 8 |
| 127 | 57 | 41 | 175 | M | 50 | 14 | 6700 | 28 |
| 169 | 56 | 69 | 168 | M | 50 | 14 | 7400 | 2 |
| 182 | 57 | 62 | 176 | M | 47 | 11 | 5200 | 8 |
| 183 | 54 | 58 | 170 | ? | 65 | 17 | 9000 | 30 |
| 183 | 64 | 86 | 172 | M | 65 | 17 | 6000 | 23 |
| 223 | 52 | 64 | 159 | M | 51 | 11 | 6900 | 15 |
| 224 | 34 | 40 | 161 | M | 50 | 17 | 5400 | 9 |
| 231 | 57 | 49 | 163 | M | 51 | 15 | 9000 | 20 |
| 232 | 57 | 49 | 163 | M | 51 | 17 | 6900 | 21 |
| 243 | 61 | 74 | 172 | M | 47 | 16 | 6500 | 6 |
| 244 | 57 | 54 | 165 | F | 50 | 16 | 5000 | 21 |
| 245 | 56 | 62 | 157 | M | 50 | 15 | 4100 | 7 |
| 246 | 62 | 52 | 165 | M | 50 | 18 | 6600 | 12 |
| 247 | 42 | 58 | 163 | M | 50 | 18 | 8900 | 8 |
| 254 | 63 | 52 | 162 | M | 50 | 17 | 9000 | 15 |
| 255 | 68 | 56 | 165 | M | 50 | 18 | 7000 | 13 |
| 256 | 48 | 87 | 180 | M | 49 | 10 | 7400 | 8 |
| 257 | 42 | 53 | 155 | F | 67 | 17 | 7500 | 14 |
| 258 | 42 | 69 | 165 | M | 66 | 15 | 7300 | 10 |
| 267 | 68 | 71 | 164 | M | 58 | 20 | 7500 | 12 |
| 268 | 62 | 66 | 172 | M | 67 | 20 | 7100 | 7 |
| 276 | 55 | 82 | 180 | M | 67 | 23 | 7800 | 20 |
| 277 | 52 | 50 | 164 | M | 68 | 18 | 6000 | 10 |
| 285 | 65 | 54 | 165 | M | 56 | 18 | 8700 | 32 |
| 286 | 47 | 74 | 170 | M | 56 | 17 | 7500 | 0 |
| 357 | 66 | 54 | 165 | M | 51 | 19 | 7200 | 26 |
| 359 | 61 | 48 | 170 | M | 50 | 21 | 5600 | 25 |
| 368 | 39 | 79 | 170 | M | 50 | 15 | 6000 | 14 |
| 372 | 37 | 60 | 160 | M | 56 | 16 | 9100 | 14 |
| 374 | 47 | 74 | 173 | M | 50 | 11 | 4400 | 4 |
| 381 | 65 | 70 | 164 | M | 50 | 12 | 7400 | 18 |
| 386 | 61 | 76 | 165 | M | 50 | 12 | 9100 | 12 |
| 6000 | 54 | 47 | 153 | F | 52 | 11 | 4600 | 10 |
| 6000 | 65 | 78 | 171 | M | 52 | 11 | 4000 | 6 |
| 9300 | 42 | 96 | 161 | M | 41 | 9 | 7000 | 10 |
| 9300 | 55 | 68 | 177 | F | 41 | 9 | 5200 | 20 |

**TableA 11: PMHS impactor tests (Kroell et al. (1971. 1974))**

| PMHS test number | Chest compression | PMHS age | Rib fractures |
|---|---|---|---|
| 12FF | 0.42 | 67 | 22 |
| 13FM | 0.44 | 81 | 21 |
| 14FF | 0.44 | 76 | 7 |
| 15FM | 0.39 | 80 | 13 |
| 18FM | 0.42 | 78 | 14 |
| 19FM | 0.38 | 19 | 1 |
| 20FM | 0.35 | 29 | 0 |
| 21FF | 0.56 | 45 | 18 |
| 22FM | 0.42 | 72 | 17 |
| 23FF | 0.43 | 58 | 23 |
| 25FM | 0.40 | 65 | 18 |
| 26FM | 0.19 | 75 | 0 |
| 28FM | 0.19 | 54 | 0 |
| 30FF | 0.31 | 52 | 3 |
| 31FM | 0.46 | 51 | 14 |
| 32FM | 0.46 | 75 | 20 |
| 34FM | 0.45 | 64 | 13 |
| 36FM | 0.35 | 52 | 7 |
| 37FM | 0.33 | 48 | 9 |
| 42FM | 0.32 | 61 | 0 |
| 45FM | 0.32 | 64 | 10 |
| 46FM | 0.31 | 46 | 0 |
| 48FM | 0.40 | 69 | 0 |
| 50FM | 0.43 | 66 | 12 |
| 51FM | 0.38 | 60 | 0 |
| 52FM | 0.49 | 65 | 11 |
| 53FM | 0.26 | 75 | 3 |
| 54FF | 0.41 | 49 | 7 |
| 55FF | 0.41 | 46 | 8 |
| 56FM | 0.39 | 65 | 3 |
| 58FM | 0.39 | 68 | 4 |
| 60FM | 0.27 | 66 | 9 |
| 62FM | 0.36 | 76 | 9 |
| 63FM | 0.37 | 53 | 4 |
| 64FM | 0.37 | 72 | 6 |

## APPENDIX B - DEFINITION OF K ANC C COEFFICIENTS FOR THE CALCULATION OF AIRBAG RELATED DEFLECTION (INDICE 1 OF FLOW CHART IN APPENDIX C)

The k and c coefficients, which better model Equation 1, were determined for each of the 12 Hybrid III sled tests with a shoulder belt restraint, from the analysis sample. For this part of the analysis, no PMHS data were needed. Therefore, 6 other Hybrid III dummy tests with a shoulder belt restraint were included. The levels of the shoulder belt load and thoracic deflection are indicated in TableA 8 and TableA 9. It is noticeable that each Hybrid III test corresponds to a single crash configuration except the tests described in TableA 7. In this case, 4 Hybrid III belt tests were performed in the same crash configuration. In order to give to these tests the same weighting as the others, the belt load and the k and c coefficients calculated were averaged. These mean values were considered to correspond to one Hybrid III test.

As it was found the k and c coefficients used in Equation 1 were constant and equal for all the belt-only restraint tests for the human body model, it was first studied if k and c coefficients constant and equal for all belt-only tests were adapted to model Equation 1 for the Hybrid III dummy. The mean and the standard deviation of these coefficients which best correspond with the relationship between the belt load and the central deflection were calculated. The means were k= 183 N/mm and c= 3 N.s/mm with standard deviations of 50 N/mm and 1.3 N.s/mm. A great dispersion of the coefficients is observed and these coefficients did not allow to model correctly Equation 1.

Horsch et al. (1991) found the dummy thoracic deflection to be dependent on the path of the belt on the shoulder and on the pelvis displacement. The influence of these parameters may explain the dispersion of the k and c coefficients. This influence could be explained by the dispersion in the belt path on the thorax with respect to the central deflection sensor, as explained farther.

A more detailed analysis of the k and c coefficients calculated showed the k and c coefficients depend on the belt load level, that is they are constant for each belt-only test but differed from one test to another according to the shoulder belt load. The relation allowing the calculation of the k and c coefficients determined was Equation B1.

$$k\text{-initial}=-0.0104*F_{belt\ max}+277 \qquad \text{(Equation B1)}$$

with k in N/mm and $F_{belt}$ in N, $R^2$=0.3.

Moreover, the analysis of the 18 Hybrid III tests showed that damping had some relation to the stiffness as shown in Equation B2.

$$c=0.0155*k+0.1916 \qquad \text{(Equation B2)}$$

with k in N/mm and c in N.s/mm, $R^2$= 0.3.

As this relationship does not allow the precise calculation of the real stiffness at the central point, some of the Hybrid III tests will present a real stiffness larger than the stiffness calculated with Equation B1, named k-initial , and some others will present a smaller stiffness.

In a Hybrid III test for which the real stiffness is larger than the one determined with k-initial, the localized deflection calculated at the central point will be larger than the measured sternal deflection for a given belt load (Figure B 1). This error can be corrected by increasing the stiffness until the difference between the localized calculated deflection and the measured sternal deflection is under 5 mm at any time. The improved stiffness is therefore named k-corrected (indice 1b of flow chart in appendix C).

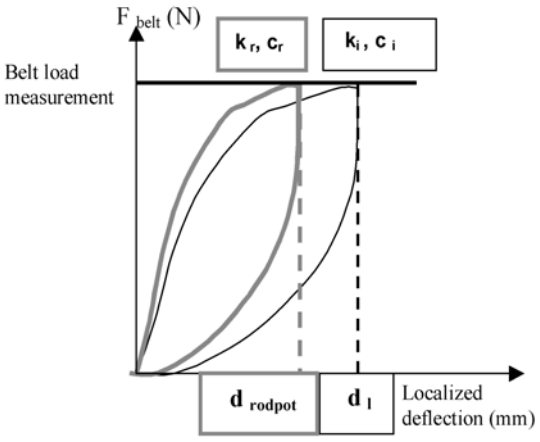


**Figure B 1: Comparison of law of behavior for the real stiffness ($k_r$, $c_r$) higher than k-initial ($k_i$, $c_i$)**

The calculated distributed deflection may become negative at certain moments, when applying the stiffness correction. It was therefore considered to be zero in order not to interfere with the calculation of the equivalent deflection.

It was also verified that the stiffness correction (k-corrected) allowed better approximation of the real stiffness (k-real) than the stiffness calculated without correction (k-initial) (Figure B 2).

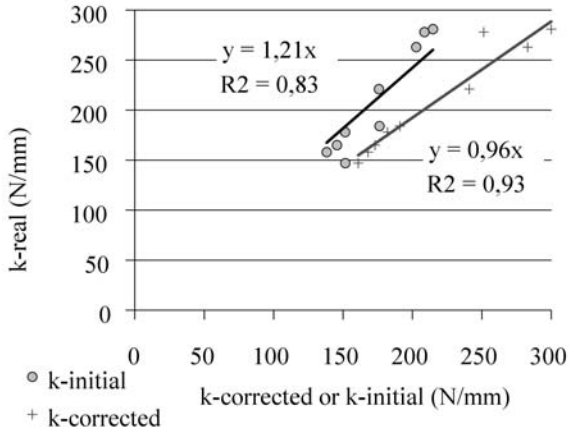


**Figure B 2: Real stiffness (k-real) as a function of the initial stiffness (k-initial) and the corrected stiffness (k-corrected)**

It was finally verified the maximal localized deflection calculated at the central point better corresponds to the maximal sternal deflection with k-corrected than with k-initial in the case of belt-only restraint (Figure B 3).

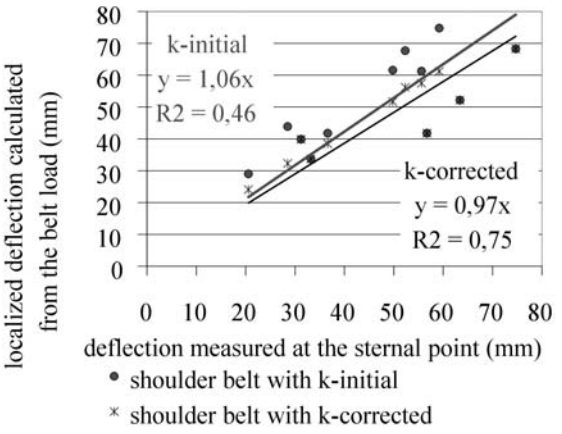


**Figure B 3: Comparison of the maximal deflection measured and of the maximal central localized deflection calculated from the belt load for Hybrid III**

This correction should also be applied for all restraints. However, it was observed that the stiffness for the combined restraints was such that this correction was never applied. For the combined restraint, the localized deflection calculated at the central point was always calculated with k-initial.

For the shoulder belt restraint with a stiffness smaller than the one determined with k-initial, the localized deflection calculated at the central point will be smaller than the sternal deflection measured. A significant distributed deflection could be erroneously calculated if the stiffness is small enough relative to the stiffness determined from the shoulder belt load. It was necessary to verify that the range of distributed deflection values calculated in this case was limited. In particular, it should be smaller than the range of distributed deflections calculated for the belt and airbag restraint. The difference between the maximal equivalent deflection and the maximal localized deflection characterizes the contribution of the distributed deflection to the risk. This was calculated for the shoulder belt and the combined restraint tests. It is presented for each Hybrid III test as a function of the maximal equivalent deflection in Figure B 4.

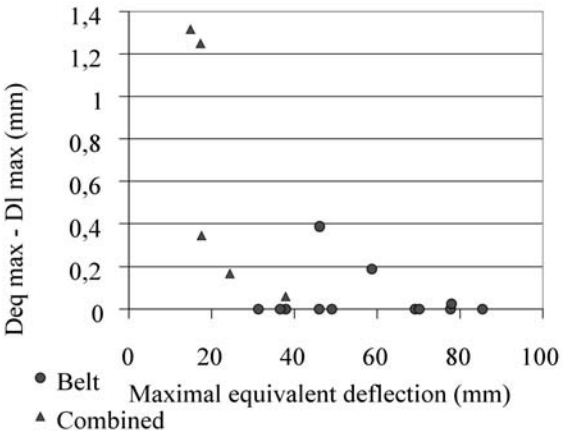


**Figure B 4: Difference between the maximal equivalent deflection ($d_{eq\ max}$) and the maximal localized deflection ($d_{l\ max}$)**

This confirms that the error concerning the relationship between the shoulder belt load and the localized deflection was limited enough to keep the contribution of the distributed deflection to the equivalent deflection negligible for most of the belt restraint tests (10 out of 12) compared to the combined restraint tests. Two belt-only tests presented some limited contribution of the distributed deflection to the equivalent deflection. This is due to the fact the stiffness k-initial calculated with Equation B1 is too small compared to the real stiffness. This may be due to the low correlation characterizing Equation B1.

**APPENDIX C – FLOW CHART OF HYBRID III CRITERION CALCULATION PROCESS**